Biogeochemistry
DOI 10.1007/s10533-014-9950-9

Combined global change effects on ecosystem processes in nine U.S. topographically complex areas

Melannie D. Hartman · Jill S. Baron · Holly A. Ewing · Kathleen C. Weathers

Received: 16 January 2013 / Accepted: 30 December 2013

Abstract Concurrent changes in climate, atmospheric nitrogen (N) deposition, and increasing levels of atmospheric carbon dioxide (CO_2) affect ecosystems in complex ways. The DayCent-Chem model was used to investigate the combined effects of these human-caused drivers of change over the period 1980–2075 at seven forested montane and two alpine watersheds in the United States. Net ecosystem production (NEP) increased linearly with increasing N deposition for six out of seven forested watersheds; warming directly increased NEP at only two of these sites. Warming reduced soil organic carbon storage at all sites by increasing heterotrophic respiration. At most sites, warming together with high N deposition increased nitrous oxide (N_2O) emissions enough to negate the greenhouse benefit of soil carbon sequestration alone, though there was a net greenhouse gas sink across nearly all sites mainly due to the effect of CO_2 fertilization and associated sequestration by plants. Over the simulation period, an increase in atmospheric CO_2 from 350 to 600 ppm was the main driver of change in net ecosystem greenhouse gas sequestration at all forested sites and one of two alpine sites, but an additional increase in CO_2 from 600 to 760 ppm produced smaller effects. Warming either increased or decreased net greenhouse gas sequestration, depending on the site. The N contribution to net ecosystem greenhouse gas sequestration averaged across forest sites was only 5–7 % and was negligible for the alpine. Stream nitrate (NO_3^-) fluxes increased sharply with N-loading, primarily at three watersheds where initial N deposition values were high relative to terrestrial N uptake capacity. The simulated results displayed fewer synergistic responses to warming, N-loading, and CO_2 fertilization than expected. Overall, simulations with DayCent-Chem suggest individual site characteristics and historical patterns of N deposition are important determinants of forest or alpine ecosystem responses to global change.

Keywords Ecosystem models · DayCent-Chem · Carbon sequestration · Greenhouse gases · Nitrogen deposition · Climate warming · Nitrate

Responsible Editor: Christopher Williams.

M. D. Hartman (✉)
Natural Resource Ecology Laboratory, Colorado State University, Fort Collins, CO 80523-1499, USA
e-mail: melannie.hartman@colostate.edu

J. S. Baron
U.S. Geological Survey, Natural Resource Ecology Laboratory, Colorado State University, Fort Collins, CO 80523-1499, USA

H. A. Ewing
Program in Environmental Studies, Bates College, Lewiston, ME 04240, USA

K. C. Weathers
Cary Institute of Ecosystem Studies, 2801 Sharon Turnpike, Millbrook, NY 12545, USA

Published online: 25 January 2014

Introduction

Natural biogeochemical cycles of carbon (C) and nitrogen (N) have been strongly altered by land-use change and human industrial and agricultural emissions, and these emissions of both are expected to increase around the world (Sutton et al. 2011). Average atmospheric carbon dioxide (CO_2) in 2008 was 385 ppm, 38 % above pre-industrial levels (Le Quéré et al. 2009), while the amount of available reactive nitrogen (Nr) in 2008 was 126 % greater than that derived from natural biological nitrogen fixation and lightning (Schlesinger 2009). Global annual N deposition is predicted to increase another two- or threefold in the coming years (Lamarque et al. 2005). Emissions of CO_2 increased nearly 30 % between 2000 and 2008, a trajectory coincident with the most carbon-intensive scenarios proposed by the Intergovernmental Panel on Climate Change (Le Quéré et al. 2009). The increase in atmospheric CO_2 is controlled not only by emissions but by the strength of terrestrial and ocean sinks for C (Canadell et al. 2007). Terrestrial ecosystems are estimated to remove nearly three gigatons (Gt) of CO_2 from the atmosphere each year, playing a strong role in carbon uptake and storage in above- and belowground biomass (Canadell and Raupach 2008). The storage capability of terrestrial biomass and soils is therefore critical to mitigating the climate change effects of increasing CO_2.

Recent papers report increased C sequestration in forests and grasslands from CO_2 and N fertilization, yet the strength of the response depends on interdependent factors that vary by location and climate, vegetation types, degree of C or N saturation, and interactions of stressors (Bedison and McNeil 2009; Campbell et al. 2009; Chen et al. 2011; Janssens and Luyssaert 2009; McMahon et al. 2010; Thomas et al. 2010). The C–N links in forests and grasslands that regulate terrestrial C storage and cycling include effects on photosynthesis from CO_2 and N stimulation, the allocation of C to above- and belowground biomass, and stimulation or suppression of microbial decomposition and respiration (Janssens and Luyssaert 2009; Liu and Greaver 2010; McMahon et al. 2010). Assessing the changes in N_2O fluxes due to enhanced Nr and warming is necessary to understand the full greenhouse gas response of forest, grassland, and agricultural systems since non-CO_2 greenhouse gas emissions can offset carbon sequestration (Schulze et al. 2009; Zaehle et al. 2011).

Empirical studies and meta-analyses of ecosystem responses to changes in climate, CO_2, and N deposition, either singly or combined, most often present results for one or two response variables. Rates of forest growth and productivity, aboveground biomass (Bedison and McNeil 2009; Boisvenue and Running 2006; McMahon et al. 2010; Thomas et al. 2010) and belowground C dynamics (de Vries et al. 2009; Liu and Greaver 2010) are among those described. Ecosystem models can offer a more comprehensive evaluation of multiple interacting or counteracting drivers and response variables (e.g. Canham et al. 2003). When validated against long-term data sets they provide a powerful way to project ecosystem responses to multiple global-change drivers and have been used to test assumptions about the direct and indirect effects of climate change on ecosystems. Studies in a northern hardwood ecosystem (Campbell et al. 2009) and coniferous forests in the Rocky Mountains (Boisvenue and Running 2010) and Austria (Eastaugh et al. 2011), for example, underscore the importance of understanding the interaction of N deposition with climatic change and the need to address spatial variability in developing scenarios about how global change will affect ecosystem processes.

Our objectives here address many of these concerns through evaluation of the coupled ecosystem and biogeochemical responses in montane and alpine ecosystems in the US to climate warming, increased or decreased atmospheric N deposition, and CO_2 fertilization. We used the ecosystem model DayCent-Chem to compare biogeochemical responses in nine primarily montane catchments across a range of US climates and N deposition histories. DayCent-Chem is a process-based ecosystem nutrient cycling model that simulates CO_2 fertilization effects while accounting for water, temperature, and nutrient N, phosphorus (P), and sulfur (S) constraints on plant growth and soil organic matter cycling (Hartman et al. 2009, 2007). We developed site-specific scenarios of climate and N deposition, under two CO_2 concentrations that represent common end-members for the likely changes in CO_2 in the next several decades. We used these scenarios to explore the relative strength of temperature, N deposition, and CO_2 as drivers of changes in C allocation to above- and below-ground biomass and soil organic matter, NEP, net greenhouse gas (GHG) flux, nitrous oxide (N_2O) emissions, and stream nitrate (NO_3^-) chemistry.

Methods

Study sites

Our study sites were instrumented watersheds from four US National Parks and four Long Term Ecological Research (LTER) areas (Table 1). The sites ranged in elevation at their outlets from 129 to 3,515 m and included two sites each from New England [Hubbard Brook LTER, NH (HBR) and Acadia National Park, ME (ACAD)], southern Appalachia [Coweeta LTER, NC (CWT) and Great Smoky Mountains National Park, NC (GRSM)], Cascades [HJ Andrews LTER, OR (HJA) and Mount Rainier National Park, WA (MORA)], and Rocky Mountains [Rocky Mountain National Park, CO (ANDCRK) and Niwot Ridge LTER, CO (NWT)] (Hartman et al. 2009). Two forested watersheds of different stand age at the HJ Andrews Experimental Forests were modeled: HJA (young) was clear-cut in 1975, and HJA (old) has trees >500 years. All sites were forested except for the Rocky Mountain locations. Detailed descriptions and model parameterization/validation for each site are found in Hartman et al. (2009).

DayCent-Chem model

DayCent-Chem is a variation of CENTURY (Hartman et al. 2007). The CENTURY models specialize in C and N cycling by incorporating detailed mechanistic representations of plant nutrient and water uptake, soil microbial activities, and soil organic matter. They have been widely applied to grasslands, forests, and agricultural lands around world (Baron et al. 1994; Parton et al. 1993, 1988, 2007). DayCent-Chem is constructed from DayCent, the daily-timestep version of CENTURY (Parton et al. 1998), and PHREEQC, a low-temperature aqueous geochemical model (Parkhurst and Appelo 1999) that allows prediction of stream and soil water chemistry for a number of solutes. A full model description is found in Hartman et al. (2007).

DayCent-Chem computes ecosystem dynamics, including soil water fluxes, snowpack and stream dynamics, plant production and nutrient uptake, litterfall, soil temperature with depth, soil organic matter decomposition, mineralization, nitrification, and denitrification, while utilizing PHREEQC's low-temperature aqueous geochemical equilibrium calculations, including CO_2 dissolution, mineral denudation, and cation exchange, to compute soil water and stream chemistry. The soil organic matter model has five soil organic pools and four litter pools described in Parton et al. (1993). The trees and grasses represented by the model are similar to plant functional types but are described by a set of site-specific parameters. Trees have five plant pools (leaves, fine branches, large wood, fine roots, and coarse roots) while grasses have two plant pools (shoots and fine roots). Inputs to DayCent-Chem include daily precipitation amount and solute concentrations, daily minimum and maximum air temperatures, and the daily dry deposition from gas, particulates, and aerosols (specified either with a dry-to-wet deposition ratio or an absolute amount of dry deposition).

Carbon and nitrogen dynamics and their response to climate, N, and CO_2 forcings

Vegetation growth dynamics and phenology in DayCent-Chem are determined by average air temperature, soil temperature, and day length. Deciduous trees begin a four-week leaf out period when day length is increasing and exceeds 10 h per day and the air temperature reaches a threshold for the plant. Deciduous leaf drop occurs when the average air temperature falls below a threshold and the day length is decreasing. The growth period for perennial and evergreen plants is determined by soil temperature. The onset of senescence for perennial plants is determined by site-specific model parameters. Elevated temperatures may shift the simulated growing season or change its length, and they will increase or reduce growing-season production as a function of the relative shift in temperature from optimal growing temperatures.

To compute actual NPP, the model first computes a maximum potential NPP (NPP_{max}, g C m^{-2} day^{-1}). This NPP_{max} is equal to the maximum production for the plant species (a model parameter) multiplied by number of calculated scaling factors that range from 0 to 2 and include the effect of self-shading, soil temperature, water availability, and atmospheric CO_2 concentration (Eq. 1) on growth (Parton et al. 1993). The soil temperature effect on growth is a Poisson density function curve with species-specific parameters that define the optimal and range of temperatures for growth.

Table 1 Site characteristics including years of measured data, catchment name, vegetation type and stand age, measured mean annual temperature, measured mean annual temperature precipitation, measured mean annual N deposition, and simulated N deposition for years 2001, 2075 (LOW N), and 2075 (HIGH N)

Site Name (abbreviation)	Years of Measured Data	Catchment	Vegetation Type (stand age)	Mean (std dev) Annual Temperature (°C)	Mean (std dev) Annual Precipitation (cm)	Mean Annual N deposition (kg N ha^{-1})	Simulated 2001 N deposition (kg N ha^{-1})	Simulated 2075 LOW N deposition (kg N ha^{-1})	Simulated 2075 HIGH N deposition (kg N ha^{-1})
Hubbard Brook LTER, NH (HBR)	1979–2004	Watershed 6	Northern mixed hardwood (~100 years)	4.4 (0.8)	142 (20)	7.0	5.5	3.9	9.6
Acadia NP, ME (ACAD)	1983–2005	Hadlock Brook	Spruce-fir (>300 years)	7.6 (0.7)	152 (32)	10.0	6.5	4.0	11.3
Coweeta LTER, NC (CWT)	1985–1995	Watershed 2	Mixed mesophytic hardwood (>100 years)	13.5 (0.7)	177 (41)	6.9	7.6	6.0	13.3
Great Smoky Mountains NP, NC (GRSM)	1981–1999	Noland Divide	Spruce-fir (>300 years)	8.6 (0.6)	232 (39)	30.6	30.0	22.1	52.4
HJ Andrews LTER, OR (HJA young)	1981–2004	Watershed 10	Douglas fir (35 years)	10.2 (0.8)	219 (44)	1.5	2.4	2.0	4.1
HJ Andrews LTER, OR (HJA old)	1981–2004		Douglas fir (>500 years)	10.2 (0.8)	219 (44)	1.5	2.4	2.0	4.1
Mount Rainier NP, WA (MORA)	1990–2007	Lake Louise	Coniferous (>300 years)	4.5 (0.5)	298 (61)	2.8	4.1	3.7	7.2
Rocky Mountain NP, CO (ANDCK)	1984–2006	Andrews Creek	Alpine (10,000 years)	−1.1 (0.5)	106 (18)	3.5	3.0	2.8	5.3
Niwot Ridge LTER, CO (NWT)	1990–2006	Green Lakes Valley	Alpine (10,000 years)	−3.1 (0.5)	124 (16)	5.9	7.2	6.9	12.7

All sites are forested except alpine ANDCK and NWT

The model dynamically computes the fraction of C to be allocated to each plant pool based on time of year and soil moisture and N availability. Initially the model moves carbon to leaves and fine roots only. This is limited to seasonal dynamics for deciduous species and to specified leaf growth periods for conifers. The fraction of C allocated to fine roots is a linear function that is a maximum (0.36 for trees and 0.70 for grasses) with low soil mineral N and low soil moisture, and is a minimum (0.30 for trees and 0.40 for grasses) when available soil mineral N equals or exceeds plant N demand and soil moisture is greater than field capacity. Based on specified ratios, C that is not allocated to leaves or fine roots is moved to large wood, branches, and coarse roots.

Species-specific model parameters define the minimum and maximum C:N ratios of each plant part based on Parton et al. (1993). Tree tissue C:N ratios are known to decrease under conditions of chronically elevated nitrogen deposition (McNulty et al. 1991). To determine when potential NPP is constrained by nutrient availability, a nutrient-limited NPP is calculated to estimate the fraction of potential NPP that can be achieved from available soil N while maintaining appropriate tissue C:N stoichiometry. The model calculates the maximum potential plant N demand (*Ndemand*, g N m^{-2} day^{-1}) by dividing NPP_{max} by the minimum C:N ratio of all plant pools. The actual N uptake rate of each plant pool (gN gC^{-1}) is a value between the minimum N:C ratio and the maximum N:C ratio of the plant pool, and N uptake varies linearly between the two N:C ratios as the quotient (available soil N)/(*Ndemand*) increases. In other words, new plant material will have a C:N ratio close to the maximum C:N when available soil N is much smaller than *Ndemand* and will have a minimum C:N ratio when available soil N is greater than or equal to *Ndemand*. The minimum and maximum C:N ratios for each plant pool vary by site. For trees they averaged 25 and 45 for leaves, 50 and 67 for fine roots, 176 and 250 for fine branches, 433 and 600 for large wood, and 250 and 384 for coarse roots. For grasses minimum and maximum C:N ratios averaged 20 and 40, respectively. These C:N ratios were increased with CO_2 fertilization as described below.

DayCent calculates a CO_2 effect on plant (primary) production, water-use efficiency, and plant C:N ratios (http://www.nrel.colostate.edu/projects/century/). Model parameters relating to CO_2 fertilization were developed for the CENTURY model during the Vegetation Ecosystem Mapping and Analysis Project (VEMAP) (Pan et al. 1998). As described in the Eqs. (1) and (2) below, the CO_2 fertilization effect was described relative to atmospheric CO_2 doubling from 350 to 700 ppm.

The potential net primary production at time t, NPP[t], was calculated as

$$\mathrm{NPP}[t] = \mathrm{NPP}[0]\left(1 + \frac{\beta_1 \log_{10}\left(\frac{\mathrm{CO_2}[t]}{\mathrm{CO_2}[0]}\right)}{\log_{10}(2)}\right), \quad (1)$$

where $\beta_1 \geq 0$, $CO_2[0] = 350$ ppm, and NPP[0] equals the potential net primary production at 350 ppm. For plant types used here, $0.20 \leq \beta_1 \leq 0.25$, meaning that a doubling of CO_2 concentration (e.g. from 350 to 700 ppm) would increase potential production by 20–25 %. Actual simulated net primary production was less than or equal to NPP[t] and depended on water and nutrient availability.

Similarly transpiration at time t, Transp[t], was reduced as CO_2 increased,

$$\mathrm{Transp}[t] = \mathrm{Transp}[0]\left(1 + \frac{\beta_2 \log_{10}\left(\frac{\mathrm{CO_2}[t]}{\mathrm{CO_2}[0]}\right)}{\log_{10}(2)}\right), \quad (2)$$

where $\beta_2 \leq 0$, $CO_2[0] = 350$ ppm, and Transp[0] is the amount of transpiration at 350 ppm. For plant types used in this exercise, $-0.25 \leq \beta_2 \leq -0.20$, which means that doubling CO_2 concentration (e.g., from 350 to 700 ppm) would decrease transpiration by 20–25 %.

In the model, site-specific vegetation parameters specify a range of allowable plant tissue C:N ratios and therefore regulate the amount of N uptake per unit of C fixed. Using a function similar to the one for NPP (Eq. 1), the model can simulate increased plant nitrogen-use efficiency (NUE). For this exercise, both minimum and maximum allowable C:N ratios of leafy and woody plant pools were set to increase by 20–25 % with a CO_2 doubling (from 350 to 700 ppm), based upon VEMAP simulations. The difference between minimum and maximum C:N ratios remained constant.

DayCent-Chem is appropriate for simulating plant- and ecosystem-level responses to CO_2 fertilization but does not compute leaf-level photosynthesis or stomatal

conductance. Models of leaf-level photosynthetic assimilation (e.g. Faquhar 1989) show that C assimilation saturates with increasing intracelluar CO_2 concentrations as photosynthesis becomes rubisco- or electron transport-limited. For DayCent-Chem, potential NPP increases logarithmically with increasing atmospheric CO_2 concentration but does not saturate (Eq. 1). However, the CO_2 effect on actual NPP may saturate due to water or N limitation. DayCent-Chem can assess positive and negative feedbacks of CO_2 fertilization at the ecosystem level. For example, increased water-use efficiency may enhance soil moisture that can increase plant production in water-limited ecosystems and/or increase soil organic matter decomposition. The CO_2 effect on NUE may allow greater C sequestration per unit of N uptake; however, the increased C:N ratio of litter inputs to the soil increases N immobilization and N available to plants.

We computed both direct soil N_2O emissions and indirect N_2O from N leaching/runoff to surface waters. The trace-gas submodel computes direct soil N_2O and nitrogen (di)oxide (NO_x) emissions as the intermediate products of denitrification and nitrification reactions (Del Grosso et al. 2000; Parton et al. 1996, 2001). The denitrification submodel assumes that N gas from denitrification is controlled by soil NO_3^-, heterotrophic CO_2 respiration (a surrogate for labile C availability), and oxygen (O_2) availability (determined by water-filled pore space and soil physical properties that control gas diffusivity). Soil nitrification rates are controlled by soil ammonium (NH_4^+) concentration, water content, soil temperature, and pH. Indirect N_2O from N leaching/runoff was calculated as 0.0075 kg N_2O–N per kg N leached runoff (IPCC/WMO/UNEP 2000). We computed cumulative N_2O emissions by summing both direct and indirect annual N_2O fluxes from 1980 to 2075. To enable comparison of sequestration of GHG (as ecosystem C accumulation in above- and below-ground biomass and SOM) with emission of GHG in the form of N_2O, we calculated the CO_2–C equivalents for N_2O flux assuming that 1 kg N_2O had the 100-year warming potential of 296 kg of CO_2 (Ramaswamy 2001).

Pre-scenario characterization of ecosystem fluxes and storage

DayCent-Chem was parameterized for each site as part of an extensive data gathering and collaborative modeling effort (Hartman et al. 2009). Model results were compared to measured ecosystem pools and fluxes, and stream chemistry. The number of measured variables available for comparison ranged from 22 for NWT and MORA to 79 for GRSM (Hartman et al. 2009).

While each of the two sites in a region were proximal to each other, pre-scenario simulations of ecosystem fluxes and C storage vary due to site-specific differences in elevation, climate, atmospheric N deposition, and stand history (Hartman et al. 2009) (Table 2). GRSM had the highest annual productivity, heterotrophic respiration, soil organic matter carbon, N mineralization, and stream NO_3^- of all sites. Other sites with high production and respiration were CWT and ACAD; all three of them are located in eastern North America. Net ecosystem production (NEP), the difference between NPP and heterotrophic respiration, was greatest at ACAD, GRSM, and HJA (old). For the alpine sites, 90 % of total ecosystem C was in belowground biomass and soil organic matter. For all forested sites except HJA (young), aboveground C was 53–66 % of total ecosystem C. The flux of N_2O from ANDCK and NWT was among the highest, and stream NO_3^- fluxes at these alpine sites were moderately high compared with the other sites. Rates of NPP, Rh, N-mineralization and N_2O flux for HJA (young) were similar to rates in HJA (old), and intermediate in rates compared with the other sites. Soil organic matter and belowground plant residue (SOM C) for the young stand was among the lowest of all sites, while NEP was among the greatest for the old-growth HJA forest. Stream NO_3^- fluxes at both HJA sites were the lowest of all sites reported. MORA was the other site with extremely low stream NO_3^-, as well as low pre-scenario rates of N mineralization and N_2O flux.

Model scenarios

We compared current with future conditions for each site under plausible increases in temperature, N deposition, and atmospheric CO_2, as described below. All treatments were adjusted gradually over the simulation period. Each site was run under "NO WARM" and "WARM," "LOW N" and "HIGH N," and "MEDIUM" and "HIGH" atmospheric CO_2 scenarios that resulted in six scenarios for each site (Table 3). We did not pair the HIGH atmospheric CO_2 concentrations with

Table 2 Mean (and standard deviation) of base ecological characteristics for each site: net primary production (NPP), heterotrophic respiration (Rh), AG-C (above ground live and dead plant material and surface plant residue), BG-C (below ground live and dead plant material and plant residue), SOM-C (below ground plant residue and partially decomposed soil organic matter), N-gas (NO_x, N_2O, N_2) flux (N-gas), net N mineralization rate (Nmin), and stream NO_3^- flux (strmNO_3^-)

Site	NPP (g C m^{-2} $year^{-1}$)	Rh (g C m^{-2} $year^{-1}$)	NEP (g C m^{-2} $year^{-1}$)	AG-C (g C m^{-2})	BG-C (g C m^{-2})	SOM-C (g C m^{-2})	Nmin (g N m^{-2} $year^{-1}$)	N-gas (g N m^{-2} $year^{-1}$)	strmNO_3^- (g N m^{-2} $year^{-1}$)
HBR (1979–2004)	414 (58)	290 (15)	124 (52)	11203 (594)	3432 (278)	4133 (85)	5.5 (0.5)	0.03 (0003)	0.70 (0.06)
ACAD (1983–2005)	567 (55)	417 (17)	150 (37)	20817 (340)	5,265 (99)	7,701 (66)	5.6 (0.3)	0.04 (0.01)	0.22 (0.08)
CWT (1985–1995)	589 (84)	538 (37)	51 (82)	11,210 (70)	3,156 (38)	5,363 (22)	7.6 (0.6)	0.16 (0.06)	0.01 (0.01)
GRSM (1981–1999)	747 (39)	621 (32)	120 (81)	27,008 (71)	3,523 (87)	11,689 (130)	9.4 (1.1)	0.13 (0.02)	1.09 (0.34)
HJA (young) (1981–2004)	402 (35)	289 (16)	114 (33)	5,579 (719)	11,395 (69)	4,940 (82)	4.2 (0.3)	0.05 (0.02)	0.03 (0.02)
HJA (old) (1981–2004)	482 (45)	357 (16)	124 (43)	35,748 (377)	12,631 (156)	5,209 (21)	5.2 (0.3)	0.07 (0.02)	0.04 (0.02)
MORA (1990–2007)	255 (63)	199 (329)	56 (48)	16,718 (96)	7,582 (109)	7,229 (29)	3.0 (0.5)	0.03 (0.01)	0.07 (0.06)
ANDCK (1984–2006)	142 (27)	149 (41)	−6 (21)	893 (18)	1,168 (15)	7,472 (30)	3.0 (0.8)	0.17 (0.04)	0.21 (0.07)
NWT (1990–2006)	109 (23)	113 (27)	−4 (9)	900 (16)	1,228 (20)	7,451 (23)	2.2 (0.6)	0.16 (0.02)	0.36 (0.07)

The years for which there are measured values are shown in parentheses in the first column

a NO WARM scenario in the same simulation. Our scenarios ran from the beginning of measured records for each site (earliest at HBR was 1979, latest at MORA was 1990) to 2075.

Each simulation had three stages: (1) a spin-up; (2) a period with measured inputs; and (3) a period with scenario inputs. The vegetation type remained constant through all three stages. The 500- to 1000- year spin-up run brought long-term C stores to quasi-equilibrium. For this stage CO_2 was set to 294 ppm, and occasional disturbance from fire or from hurricane blow down was simulated based on the site's history. The measured meteorological record for the site, which was much shorter than 100 years, was repeated many times, and N deposition was set at background levels (0.5 kg N ha^{-1} $year^{-1}$) (Holland et al. 1999) until simulation year 1900 when N deposition was ramped linearly to reach measured amounts. HJA (young) was spun up as for HJA (old) site until 1975, when 95 % of above-ground biomass was removed. For the next stage, the model was driven by measured atmospheric deposition, daily weather, and CO_2 concentrations; this stage started sometime between 1979 and 1990, depending on data availability for each site and ended with simulation year 2000. Simulations for years 2001–2075 were driven by the scenarios in daily climate, N deposition, and atmospheric CO_2. The six simulations for each site were identical from the start of the spin-up to the end of year 2000 before they branched off into the scenario inputs in 2001.

Climate scenarios for 2001–2075

Climate warming (WARM) scenarios were taken from Leung and Qian (2005). The scenarios were derived from MM5 (Penn State/NCAR Mesoscale Model) downscaled projections of the NCAR/DOE Parallel Climate Model (PCM) for 1976–2075 (Leung and Qian 2005; Leung et al. 2003). Control runs came from a 1975–1996 PCM simulation of historical climate using historical greenhouse gas emissions. Future climate PCM runs were initiated in 1995 with ocean data assimilation and a business-as-usual emissions scenario for greenhouse gases and aerosols, which produced about 1 % increase in greenhouse gas concentrations per year. MM5 is a regional climate model that was used to dynamically downscale control and future simulations using a nested model configuration that yielded climate at 36 km spatial

Table 3 The six scenarios of N deposition, climate, and atmospheric CO_2 concentrations

	LOW N WARM MED CO_2	LOW N NO WARM MED CO_2	LOW N WARM HIGH CO_2	HIGH N WARM MED CO_2	HIGH N NO WARM MED CO_2	HIGH N WARM HIGH CO_2
N deposition 2001–2075	CAIR to 2020, then constant	CAIR to 2020, then constant	CAIR to 2020, then constant	increased 1 % annually	increased 1 % annually	increased 1 % annually
Climate 2001–2075	MM5, 2–3 °C warming	historic, randomized years, no temperature trend	MM5, 2–3 °C warming	MM5, 2–3 °C warming	historic, randomized years, no temperature trend	MM5, 2–3 °C warming
CO_2 concentration year 2075 (ppm)	600	600	760	600	600	760

N deposition and climate were site-specific. Observed N deposition, weather, and CO_2 concentrations were used to drive the model prior to 2001. Low N deposition (LOW N) after 2001 was based on expected deposition with implementation of the Clean Air Interstate Rule (CAIR). High N deposition (HIGH N) scenarios added 1 % of the site's 2001 N deposition amount each year. MM5 is the Penn State/NCAR Mesoscale Model downscaled climate predictions for 2001–2075. Atmospheric CO_2 concentrations were increased from the measured value in 2001 to medium concentrations (MED CO_2) based on the IPCC IS92a business-as-usual projections (IPCC 1996) or high concentrations (HIGH CO_2) based on CO_2 scenarios from A1F1, the highest SRES CO2 emissions scenario (Nakicenovic et al. 2000)

resolution. Climate files were extracted based on latitude and longitude from the larger data set. Meteorological data measured at each site were compared to MM5 climate files for overlapping years. MM5 daily temperatures and precipitation were systematically adjusted using Eqs. 3–6 across all years (including those beyond the instrumental record) so that there was a match between the years of measurement and the early model years and the resulting annual means were consistent with observed weather.

To compute daily scenario temperatures ($Tscen_{daily}$), ΔT was calculated as the average difference between mean annual observed temperature ($Tobs_{annual}$) and mean annual MM5 temperature ($TMM5_{annual}$), where n is the number of years observations were available. This procedure was done separately for minimum and maximum air temperatures.

$$\Delta T = \frac{1}{n}\sum (Tobs_{annual} - TMM5_{annual}) \quad (\text{for years } 1976-2005) \tag{3}$$

$$Tscen_{daily} = TMM5_{daily} + \Delta T \ (\text{for years } 2001-2075) \tag{4}$$

To compute daily scenario precipitation (Pscendaily), ΔP was calculated as the average annual ratio of annual observed precipitation ($Pobs_{annual}$) to annual MM5 precipitation ($PMM5_{annual}$), where n is the number of years observations available.

$$\Delta P = \frac{1}{n}\sum \frac{Pobs_{annual}}{PMM5_{annual}} \ (\text{for years } 1976-2005) \tag{5}$$

$$Pscen_{daily} = \Delta P \times PMM5_{daily} (\text{for years } 2001-2075) \tag{6}$$

The resulting WARM scenarios for all sites showed a 0.02–0.03 °C $year^{-1}$ increase in average annual temperature, resulting in a 2–3 °C increase by 2075, depending on the site.

Each site-specific NO WARM scenario was derived from observed weather by randomly shuffling and repeating year-long segments of daily meteorological records. The NO WARM scenario had no temperature trend. For all sites, the difference in annual mean precipitation between the WARM and NO WARM scenarios was not significantly different, and neither scenario showed a decline or increase in annual precipitation over time.

Nitrogen scenarios for 2001–2075

All simulations used site-specific measured and modeled total inorganic N deposition (CASTNET 2009; NADP/NTN 2009; other data sources listed in Hartman et al. (2009)) through 2000. We did not consider

the effects of S deposition in this study. Site-specific LOW N or HIGH N deposition scenarios were applied from 2001 to 2075 (Table 1). The LOW N deposition scenarios were based on U.S. EPA projections of deposition of wet and dry inorganic N species simulated for 36-km grid cells across the U.S. by the U.S. EPA Community Multiscale Air Quality (CMAQ v4.5) Modeling System (http://www.cmaq-model.org/). CMAQ provided a '2001 Base Case', that was validated against measurements, and the total annual deposition of each chemical species for 2010, 2015, 2020 based on projected effects of the EPA Clean Air Interstate Rule, CAIR, which caps sulfur dioxide (SO_2) and NO_x emissions. Daily wet and dry deposition inputs were created with linear interpolation of annual deposition amounts for the years between 2001, 2010, 2015, and 2020. Deposition amounts from 2020 were applied to each subsequent year to 2075. Daily deposition was calculated as annual deposition divided by 365. We scaled up the 2001, 2010, 2015, and 2020 N deposition amounts in the CMAQ scenario for two sites, GRSM and NWT, because CMAQ simulated deposition in 2001 was much lower than measured 2001. The adjustments were made by scaling CMAQ results to match measured results, and that scalar was then applied to all subsequent years for each chemical solute.

The HIGH N scenario was created by increasing annual simulated 2001 deposition amounts by 1 % each year to 2075. After 75 years annual deposition was 1.75 times as great as it was simulated to be in 2001. Daily deposition amounts were the annual amount divided by 365.

Atmospheric CO_2 scenarios

Atmospheric CO_2 concentration was equal to the annual mean measured concentration at Mauna Loa for all scenarios and all sites through simulation year 2000 (for example, 339 ppm in 1980 and 369.4 ppm in 2000, http.cmdl.noaa.gov/ccg/co2/trends/co2_annmean_mlo.txt). Starting with year 2001, annual atmospheric CO_2 concentrations were ramped to one of two potential future concentrations. For two of the six simulations, the 2075 CO_2 concentration reached 760 ppm. This "HIGH CO_2" scenario was based on A1F1, the highest CO_2 emissions scenario from the Special Report on Emissions Scenarios (SRES) (Nakicenovic et al. 2000). For the other four simulations, the 2075 CO_2 concentration reached 600 ppm. This "MEDIUM CO_2" scenario was based on the older IPCC IS92a business-as-usual projection (IPCC 1996) which was in the middle of the range of SRES atmospheric CO_2 projections. CO_2 concentrations were incremented annually by a constant amount in order to reach either 760 or 600 ppm.

According to Eq. (1) with $\beta_1 = 0.25$, when CO_2 is at 760 ppm, potential NPP would be 7 % greater than when CO_2 is at 600 ppm. Further, the cumulative potential increase in NPP over 75 years would be 4.6 % greater for HIGH CO_2 than for MEDIUM CO_2, and it would be 9 % greater for MEDIUM CO_2 compared to a constant concentration of 369.4 ppm. However, actual NPP is still limited by day length, temperature, soil moisture, self-shading, and nutrient availability. The equivalent increases in water use efficiency (Eq. 2) and nitrogen use efficiency (described above) could enhance production or lead to ecosystem-level feedbacks that limit production depending on site-specific conditions.

Calculated response variables

Mean percent differences

The mean percent differences between responses to individual scenarios for above- and below-ground live biomass C, SOM C, N-gas flux, N mineralization rate, and stream NO_3^- flux were calculated by subtracting the percent changes from base conditions for the last ten years of simulations (2065–2075) (Tables 4, 6) for pairs of scenarios, then averaging the differences for HIGH N minus LOW N, WARM minus NO WARM, and HIGH CO_2 minus MEDIUM CO_2 scenarios. For example, the mean percent difference for HIGH N–LOW N was computed by (1) subtracting the percent change from base conditions for LOW N NO WARM from the percent change for HIGH N NO WARM (2) subtracting the percent change from base conditions for LOW N WARM from the percent change for HIGH N WARM, then (3) averaging these two differences.

Response ratios

Response ratios for each site and scenario were calculated to compare the effect of different

Table 4 Carbon pools

	LOW N NO WARM MED CO_2	LOW N WARM MED CO_2	HIGH N NO WARM MED CO_2	HIGH N WARM MED CO_2	LOW N WARM HIGH CO_2	HIGH N WARM HIGH CO_2
HBR						
AG-C	14,602 (30)	16,737 (49)	16,830 (50)	18,215 (63)	16,959 (51)	18,515 (65)
BG-C	4,823 (41)	4,972 (45)	4,799 (40)	5,167 (51)	4,975 (45)	5,250 (53)
SOM-C	4,294 (4)	4,398 (6)	4,775 (16)	4,512 (9)	4,423 (7)	4,505 (9)
ACAD						
AG-C	22,013 (6)	22,902 (10)	23,716 (14)	24,724 (19)	22,989 (10)	24,798 (19)
BG-C	5,559 (6)	5,837 (11)	5,962 (13)	6,291 (20)	5,866 (11)	6,316 (20)
SOM-C	8,030 (4)	7,542 (−2)	8,246 (7)	7,823 (2)	7,543 (-2)	7,810 (1)
CWT						
AG-C	13,512 (21)	13,575 (21)	15,373 (37)	15,405 (37)	13,608 (21)	15,431 (38)
BG-C	4,031 (28)	4,012 (27)	4,935 (56)	4,903 (55)	4,018 (27)	4,908 (56)
SOM-C	5,704 (6)	5,539 (3)	6,094 (14)	5,891 (10)	5,519 (3)	5,877 (10)
GRSM						
AG-C	27,344 (1)	27,274 (1)	27,781 (3)	27,708 (3)	27,375 (1)	27,810 (3)
BG-C	3,555 (1)	3,623 (3)	3,601 (2)	3,667 (4)	3,638 (3)	3,681 (4)
SOM-C	11,958 (2)	11,476 (−2)	12,002 (3)	11,518 (-2)	11,454 (-2)	11,498 (-2)
HJA (young)						
AG-C	15,783 (183)	14,769 (165)	16,790 (201)	15,603 (180)	14,998 (169)	15,846 (184)
BG-C	12,346 (8)	11,608 (2)	13,015 (14)	12,157 (7)	11,748 (3)	12,304 (8)
SOM-C	4,877 (−1)	4,638 (-6)	4,992 (1)	4,728 (−4)	4,661 (−5)	4,753 (−3)
HJA (old)						
AG-C	41,048 (15)	39,763 (11)	42,055 (18)	40,606 (14)	40,000 (12)	40,878 (14)
BG-C	14,579 (15)	13,755 (9)	15,247 (21)	14,306 (13)	13,898 (10)	14,476 (15)
SOM-C	5,532 (6)	5,265 (1)	5,644 (8)	5,354 (3)	5,288 (2)	5,380 (3)
MORA						
AG-C	18,507 (11)	19,407 (16)	19,578 (17)	20,449 (22)	19,506 (17)	20,550 (23)
BG-C	9,025 (19)	9,495 (25)	9,355 (23)	9,817 (30)	9,536 (26)	9,859 (30)
SOM-C	7,776 (8)	7,534 (4)	8,091 (12)	7,825 (8)	7,537 (4)	7,828 (8)
ANDCK						
AG-C	945 (6)	844 (−5)	1,013 (13)	882 (−1)	850 (−5)	893 (0)
BG-C	1,288 (10)	1,334 (14)	1,322 (13)	1,364 (17)	1,444 (24)	1,468 (26)
SOM-C	7,459 (0)	6,795 (−9)	7,525 (1)	6,853 (−9)	6,943 (−7)	7,010 (−6)
NWT						
AG-C	1,261 (40)	1,148 (28)	1,338 (49)	1,224 (36)	1,134 (26)	1,214 (35)
BG-C	1,342 (9)	1,647 (34)	1,373 (12)	1,687 (37)	1,722 (40)	1,764 (44)
SOM-C	7,603 (2)	7,280 (−2)	7,644 (3)	7,356 (−1)	7,344 (−1)	7,424 (0)

Above ground C (AG-C), below ground C (BG-C), and total soil organic matter C (SOM-C) (g C m^{-2}) in 2075 for the six scenarios (% difference from base values from Table 2). ABOVEGROUND C includes above ground live and dead plant material and surface plant residue. BELOWGROUND C includes below ground live and dead plant material and plant residue. SOM C includes below ground plant residue and partially decomposed soil organic matter

treatments on total ecosystem C content from the beginning to end of the simulations. The response ratios were determined by dividing total ecosystem C at year 2075 (less the CO_2–C equivalent lost as N_2O from 2001 to 2075) by total ecosystem C at base conditions.

Nitrogen use efficiency

We also calculated metrics for NUE and net ecosystem greenhouse gas (GHG) flux. Nitrogen use efficiency (NUE, g C g N^{-1}), the increase in NEP (g C) for every 1 g increase in N deposition, was calculated as the slope of regression line when NEP was plotted against N deposition. We considered NUE only for the HIGH N scenarios; for each LOW N scenario the amount of N deposition was nearly constant throughout the simulation.

Net ecosystem greenhouse gas flux

We computed the net ecosystem GHG flux by subtracting cumulative N_2O emissions expressed as CO_2-C equivalents (g CO_2–Ce m^{-2}) from 1980 to 2075 from total ecosystem C accumulation (aboveground C, belowground C, and SOM C, g C m^{-2}) over the same period. Positive values identified terrestrial systems that were net GHG sinks, and negative values those that were a net GHG source.

Results

We focus here on (1) whether ecosystem responses revealed synergistic interaction among N deposition, warming, and elevated CO_2 as drivers of change, (2) whether there were differences in the magnitude of ecosystem responses over the course of the simulation as a function of the driving factors N deposition, warming, and CO_2, and (3) how site-specific characteristics affected ecosystem responses.

Aboveground biomass C responses to individual and cumulative drivers

Once the baseline C accumulation over time was factored out, N deposition and warming appeared to have the greatest supplemental effect on aboveground C (aboveground live and dead plant material and plant residue) accumulation in these systems. When the aboveground C values were compared among the base conditions (Table 2) and the model output from 2075 for the different scenarios (Table 4), aboveground C was seen to have increased over base values. The increase in aboveground C was small for GRSM and ANDCK, and greatest in the aggrading forest, HJA (young). HIGH N stimulated aboveground C accrual at all sites, with the greatest stimulation of HIGH N over LOW N at HBR, CWT, and HJA (young) (Fig. 1). Aboveground C was also stimulated with WARM scenarios at HBR, but had a negligible or negative response at all other sites. At HJA (young) and the two alpine sites WARM scenarios reduced the amount of aboveground C accumulation compared with NO WARM by 10–20 % (Fig. 1).

Aboveground biomass C production was greater in the HIGH N WARM scenario than scenarios of either HIGH N or WARM alone but only at those forest sites with the lowest annual mean temperature: HBR, ACAD, and MORA (Table 4). For all other sites there was no enhanced response. The difference in aboveground C accumulation between the MEDIUM CO_2 and HIGH CO_2 scenarios was <5 % for all sites (Fig. 1).

Belowground biomass C responses to individual and cumulative drivers

Across sites, belowground biomass C responses were generally smaller percentages of the baseline than aboveground biomass responses and no single driving factor stood out as responsible for large changes. Belowground biomass C increased from base conditions to 2075 in all scenarios, but the absolute amount of increase was slight for GRSM and the two alpine sites (Tables 2, 4). There was a dramatic increase in belowground C (belowground live and dead plant material and plant residue) at CWT in response to HIGH N compared with LOW N, but the influence of HIGH N was less than 10 % at all other sites (Fig. 1). WARM scenarios stimulated below-ground production at the expense of above-ground production at the two alpine sites (Fig. 1). WARM scenarios stimulated 29 % greater belowground C accumulation at NWT and 9 % at ANDCRK and HBR, but the difference in belowground C accrual between WARM and NO WARM was not large at other sites, with slightly greater accumulation from warming at some, and slightly less overall accumulation at both young and old HJA sites. As with aboveground biomass C production, belowground biomass C was stimulated by HIGH N WARM, at those forest sites with the lowest mean annual temperatures and also at the two alpine sites. Belowground biomass C was stimulated by 9 and 6 % at ANDCK and NWT, respectively, by

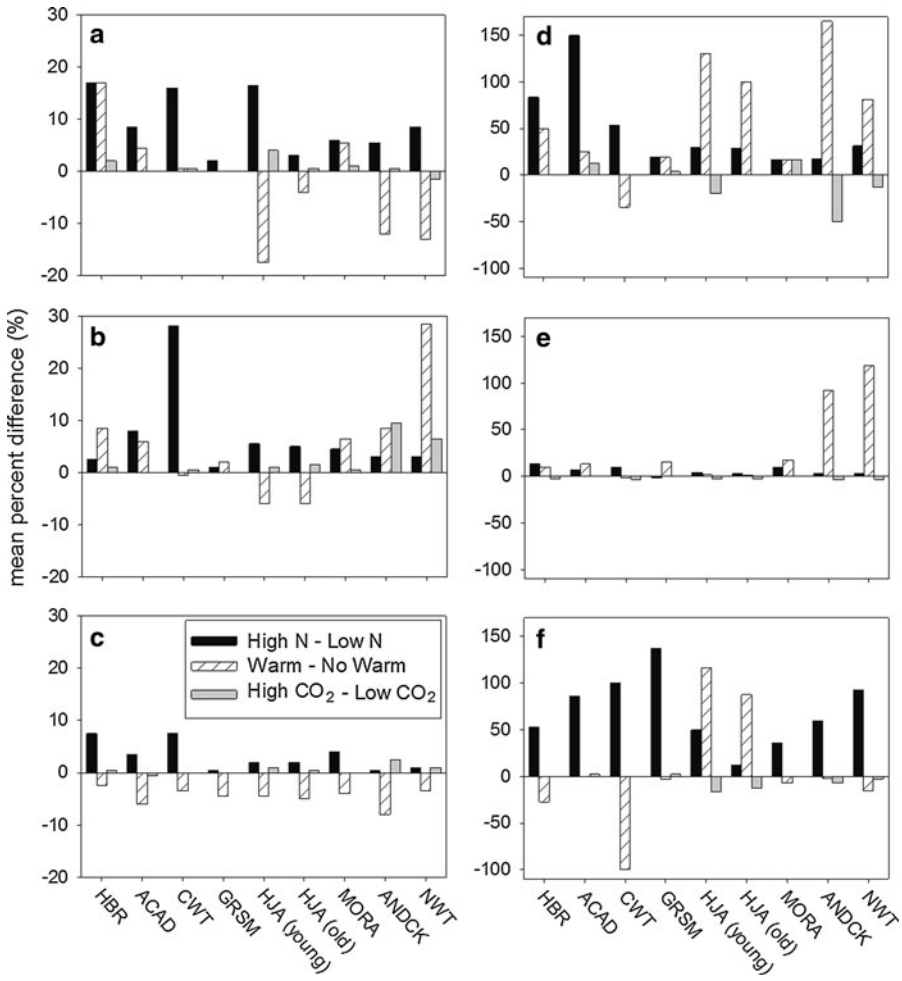

Fig. 1 The mean difference in percent change from base conditions for the last 10 years of simulations (2065–2075) between HIGH N and LOW N, WARM and NO WARM, and HIGH CO_2 and MED CO_2 scenarios. **a** Above ground carbon; **b** below ground carbon; **c** soil organic matter carbon; **d** Total N-gas ($N_2O + NO_x + N_2$) emissions; **e** net N mineralization; **f** stream nitrate fluxes. A negative value indicates a flux to the atmosphere or a loss from the ecosystem; a positive value indicates sequestration

the HIGH CO_2 scenarios, but there was negligible response to CO_2 at any other site (Fig. 1).

Soil organic matter C responses to individual and cumulative drivers

Soil organic matter C either increased slightly, decreased slightly, or did not change from base conditions over the simulations (Tables 2, 4), and most sites showed little response to the drivers (Fig. 1). HIGH N scenarios stimulated SOM C at all forested sites except GRSM. WARM scenarios decreased SOM C at all sites. There was very little response in SOM C to the HIGH CO_2 scenario. The greatest enhancement of SOM over baseline conditions occurred with HIGH N NO WARM at all sites. HJA (young), which had a large amount of litter from a 1975 clearcut, had a net loss SOM C for all scenarios.

Trends in net ecosystem production

Net ecosystem production fluctuated with precipitation and air temperature over the simulation period, but there was significant change in NEP either over time or with treatments at only half of the sites (Fig. 2; Table 5). Most sites showed modest gains in NEP under some scenarios by 2075, but the alpine sites had slightly negative NEP for some scenarios. Positive responses in NPP or Rh to N, warming, and CO_2, while often statistically significant, appeared to cancel each other out (Table 5). HIGH N scenarios showed the greatest gain (0.86–1.02 g C m^{-2} $year^{-1}$) in NEP, particularly at CWT, HJA (young) and HJA (old) compared with the LOW N scenarios (0.41–0.43 g C m^{-2} $year^{-1}$). NEP at GRSM responded to WARM scenarios. Only two forests, ACAD and MORA, showed greater NEP specifically in response to HIGH N WARM. There

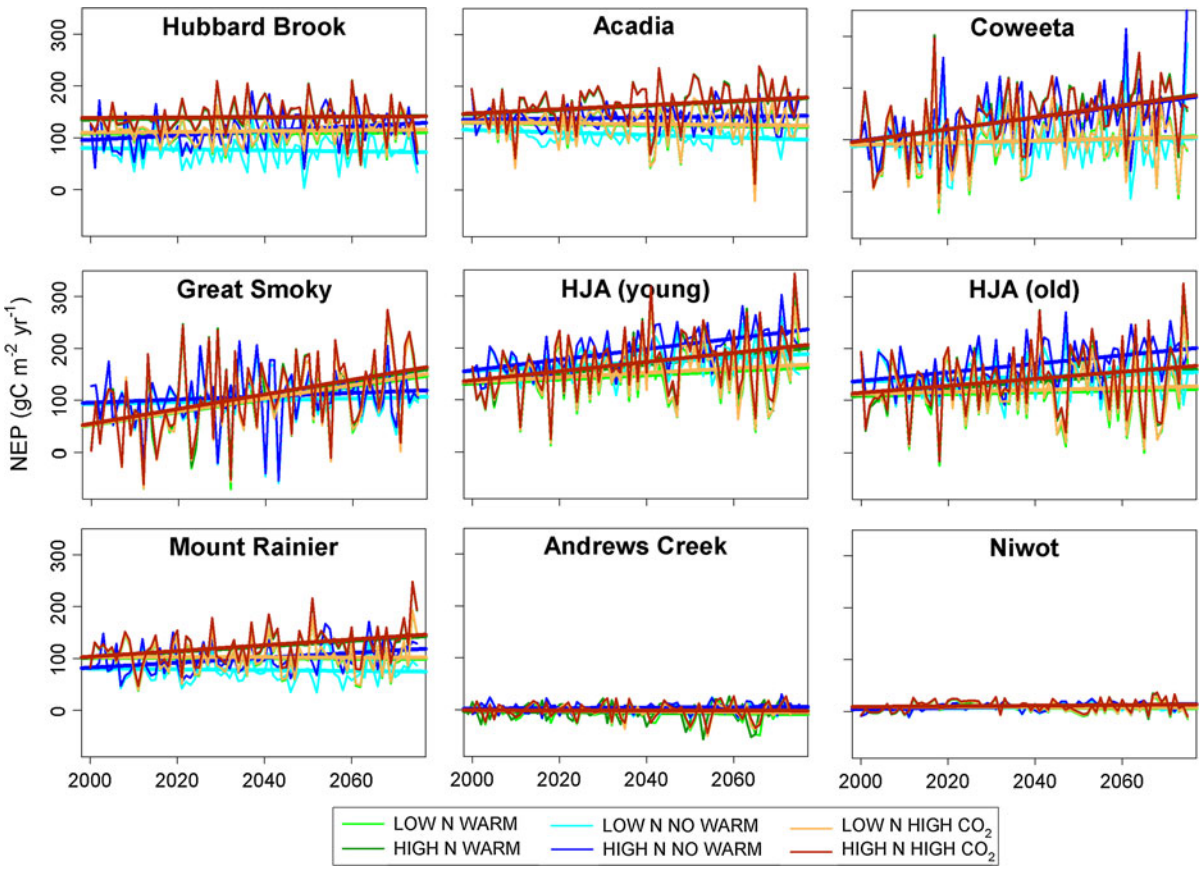

Fig. 2 Simulated annual Net Ecosystem Production (NEP) and trends from 2000 to 2075 for all sites and all scenarios (g C m^{-2} $year^{-1}$)

were no significant changes in NEP with any scenario for HBR, ANDCK, or NWT. The NEP responses to HIGH CO_2 scenarios were not much different than NEP responses to their MEDIUM CO_2 counterparts.

Nitrogen use efficiency

For most sites, NUE values were higher with warming than with no warming (Fig. 3). However, this was not the case for HBR and the two alpine sites. The alpine sites did not respond to increases in N. Among forests, NUE values were lowest for the sites with initially high N deposition (HBR, ACAD, GRSM) and were highest at both Young and Old HJA sites, where N deposition was initially lowest.

Nitrogen mineralization rates

HIGH N increased N mineralization at some, but not all, forested sites. GRSM and the two HJA sites were the least responsive to HIGH N (Fig. 1). Nitrogen mineralization rates increased strongly under WARM scenarios in the alpine and less so at most forested sites (Table 6). HIGH CO_2 had little effect on N mineralization. As with above- and belowground biomass C production, increased mineralization in response to HIGH N WARM was observed at HBR, ACAD, and MORA, the forested sites with low mean annual temperatures. At any given site, the magnitude of change in rates of mineralization and soil organic matter decomposition (indicated by modeled Rh) were similar in response to warming and N deposition.

N_2O, NO_x, and N_2 emissions

Total N gas (N_2O + NO_x + N_2) emissions from soils ranged from a low of 0.03 g N m^{-2} $year^{-1}$ at HBR and MORA to a high of 0.70 g N m^{-2} $year^{-1}$ at GRSM (Table 6). Sites fell into two categories in terms of which driving variable caused the greatest

Table 5 Slopes (average increase per year) of net primary production (NPP), heterotrophic respiration (Rh), and net ecosystem production (NEP) (g C m^{-2} $year^{-1}$ $year^{-1}$) for each site and scenario from 2001 to 2075

	LOW N NO WARM			LOW N WARM			HIGH N NO WARM			HIGH N WARM			LOW N WARM			HIGH N WARM		
	MED CO_2			MED CO_2			MED CO_2			MED CO_2			HIGH CO_2			HIGH CO_2		
SITE	NPP	Rh	NEP	NPP	Rh	NEP	NPP	Rh	NEP	NPP	Rh	NEP	NPP	Rh	NEP	NPP	Rh	NEP
HBR	0.36	0.46*	−0.1	0.84*	0.81*	0.03	1.48*	1.06*	0.42	1.05*	0.97*	0.09	0.94*	0.86*	0.07	1.00*	0.96*	0.03
ACAD	−0.02*	0.22*	−0.24	0.31*	0.41*	−0.10	0.55*	0.45*	0.10	1.20*	0.80*	0.40	0.37*	0.45*	−0.08	1.22*	0.81*	0.40
CWT	0.71*	0.51*	0.19	1.03*	0.80*	0.23	2.43*	1.34*	1.09*	2.79*	1.61*	1.18*	0.96*	0.77*	0.19	2.73*	1.59*	1.14*
GRSM	0.15	−0.03	0.18	1.79*	0.56*	1.23	0.31	0.00	0.31	1.97*	0.59*	1.37*	1.94*	0.67*	1.27	2.12*	0.71*	1.41*
HJA (young)	0.78*	0.35*	0.43*	0.69*	0.28*	0.41*	1.58*	0.55*	1.02*	1.31*	0.45*	0.86*	0.74*	0.31*	0.43*	1.37*	0.48*	0.89*
HJA (old)	0.62*	0.39*	0.23	0.51	0.34*	0.18	1.40*	0.58*	0.82*	1.13*	0.50*	0.63	0.54	0.36*	0.19	1.20*	0.52*	0.68
MORA	0.19	0.27*	−0.08	0.53*	0.55*	−0.02*	0.97*	0.49*	0.47*	1.33*	0.79*	0.53*	0.60*	0.61*	−0.01	1.40*	0.85*	0.55*
ANDCRK	−0.12	−0.10	−0.01	0.92*	0.99*	−0.07	0.00*	−0.04	0.05	1.06*	1.09*	−0.03	1.10*	1.16*	−0.06	1.23*	1.25*	−0.02
NWT	0.07	0.01	0.06	1.40*	1.42*	−0.02	0.18*	0.05	0.13*	1.59*	1.53*	0.05	1.47*	1.49*	−0.02	1.67*	1.61*	0.06

Significant trends ($p \leq 0.01$) are noted with *.

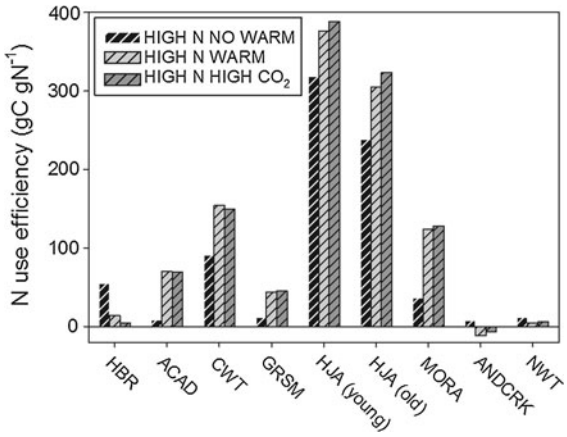

Fig. 3 Nitrogen use efficiency (NUE, g C g N^{-1}), the increase in NEP (g C) for every 1 g increase in N deposition, for High N deposition scenarios. NUE was calculated as the slope of regression line when NEP was plotted against N deposition

response: (1) western sites where the largest cumulative change in N_2O emissions was due to warming and (2) eastern sites where increases in N_2O emissions were greatest in scenarios with high N deposition, often in combination with warming (Fig. 4). For four of the western sites (HJA (young), HJA (old), ANDCK, and NWT) N_2O emissions were greater with both HIGH N WARM than with either HIGH N or WARM alone. Both HIGH N and WARM individually stimulated N_2O production at all sites. The influence of HIGH CO_2 was slight at most sites. HIGH CO_2 depressed N_2O production compared with MEDIUM CO_2 slightly at HJA (young), HJA (old), ANDCK, and NWT (Fig. 4), and depressed total N-gas flux by 20 % at HJA (young) and 50 % at ANDCK (Fig. 1). The CO_2–C equivalents (CO_2–Ce) from cumulative direct plus indirect N_2O flux, which were all positive fluxes to the atmosphere, ranged from 121 to 864 g CO_2–Ce m^{-2}. These were of roughly the same magnitude as the change in SOM C (which ranged from −720 to +858 g CO_2–C m^{-2}) over the simulation period (Fig. 4). MORA, the site with the lowest N_2O flux, was the only watershed with greater soil C storage than CO_2–Ce emissions due to N_2O for all scenarios.

Stream nitrate

Stream NO_3^- fluxes were positively related to HIGH N at all sites, and increased with the WARM scenarios only at HJA(young) and HJA (old) (Table 6; Fig. 1).

Table 6 Nitrogen fluxes

	LOW N NO WARM		LOW N WARM		HIGH N NO WARM		HIGH N WARM		LOW N WARM		HIGH N WARM	
	MED CO_2		MED CO_2		MED CO_2		MED CO_2		HIGH CO_2		HIGH CO_2	
	Mean (sd)	% diff	Mean (sd)	% diff	Mean (sd)	% diff	Mean (sd)	% diff	Mean (sd)	% diff	Mean (sd)	% diff
HBR												
N-gas	0.03 (0.0)	0	0.04 (0.0)	33.3	0.05 (0.0)	66.7	0.07 (0.0)	133.3	0.04 (0.0)	33.3	0.07 (0.0)	133.3
Nmin	5.1 (0.3)	−6.5	5.9 (0.3)	7.8	6.1 (0.3)	11.1	6.4(0.3)	16.5	5.8 (0.3)	6.2	6.23(0.3)	13.3
strmNO_3^-	0.1 (0.1)	−35	0.1 (0.0)	−60	0.2 (0.1)	20	0.2 (0.1)	−10	0.1 (0.0)	−60	0.2 (0.1)	−10
ACAD												
N-gas	0.05 (0.0)	25	0.07 (0.0)	75	0.12 (0.0)	200	0.12 (0.0)	200	0.08 (0.0)	100	0.12 (0.1)	200
Nmin	5.6 (0.3)	0.4	6.3 (0.3)	13.2	6.0 (0.3)	7.3	6.8 (0.4)	20.5	6.3 (0.3)	13.2	6.8 (0.0)	20.5
strmNO_3^-	0.2 (0.1)	−27.3	0.2 (0.1)	−27.3	0.4 (0.1)	59.1	0.4 (0.1)	59.1	0.2 (0.1)	−27.3	0.4 (0.1)	63.6
CWT												
N-gas	0.22 (0.1)	37.5	0.15 (0.0)	−6.3	0.29 (0.0)	81.2	0.25 (0.0)	56.3	0.15 (0.0)	−6.3	0.25 (0.0)	56.2
Nmin	7.6 (0.3)	0	7.5 (0.4)	−1.3	8.4 (0.3)	10	8.2 (0.5)	8.4	7.2 (0.4)	−4.6	8.0 (0.4)	5
strmNO_3^-	<0.1 (0.0)	100	<0.1 (0.0)	0	<0.1 (0.0)	200	<0.1 (0.0)	100	<0.1 (0.0)	0	<0.1 (0.0)	100
GRSM												
N-gas	0.15 (0.0)	15.4	0.17 (0.0)	30.8	0.17 (0.0)	30.8	0.20 (0.0)	53.8	0.18 (0.0)	38.5	0.20 (0.0)	53.8
Nmin	10.7 (0.7)	14	12.1 (1.0)	28.7	10.5 (0.2)	11.9	12.0 (0.2)	27.8	12.1 (1.0)	28.7	12.0 (1.0)	27.7
strmNO_3^-	1.1 (0.1)	2.8	1.1 (0.1)	−1.8	2.6 (0.3)	138.5	2.6 (0.3)	137	1.1 (0.1)	0	2.6 (0.2)	139.4
HJA (young)												
N-gas	0.06 (0.0)	20	0.12 (0.0)	140	0.07 (0.0)	40	0.14 (0.0)	180	0.11 (0.0)	120	0.13 (0.0)	160
Nmin	4.8 (0.3)	15	4. (0.4)	16.4	5.0 (0.3)	18.8	5.1 (0.4)	20.5	4.8 (0.4)	13.8	4.9 (0.4)	17.1
strmNO_3^-	<0.1 (0.0)	−33.3	0.1 (0.0)	66.7	<0.1 (0.0)	0	0.1 (0.0)	133.3	0.1 (0.0)	66.7	0.1 (0.0)	100
HJA (old)												
N-gas	0.07 (0.0)	0	0.13 (0.0)	85.7	0.08 (0.0)	14.3	0.16 (0.0)	128.6	0.13 (0.0)	85.7	0.16 (0.0)	128.6
Nmin	5.1 (0.3)	−1.3	5.2 (0.4)	0.2	5.3 (0.4)	2.1	5.4 (0.4)	3.1	5.1 (0.4)	−2.1	5.2 (0.4)	0.6
strmNO_3^-	<0.1 (0.0)	−25	0.1 (0.0)	50	<0.1 (0.0)	−25	0.1 (0.0)	75	0.1 (0.0)	50	0.1 (0.0)	50
MORA												
N-gas	0.03 (0.0)	0	0.04 (0.0)	33.3	0.04 (0.0)	33.3	0.04 (0.0)	33.3	0.04 (0.0)	33.3	0.05 (0.0)	66.7
Nmin	3.3 (0.4)	9	3.8 (0.6)	26.3	3.6 (0.4)	18.7	4.1 (0.6)	36.3	3.8 (0.6)	26.7	4.09 (0.61)	36.3
strmNO_3^-	0.1 (0.1)	14.3	0.1 (0.1)	0	0.1 (0.1)	42.9	0.1 (0.1)	42.9	0.1 (0.1)	0	0.1 (0.1)	42.9
ANDCK												
N-gas	0.15 (0.0)	−11.8	0.42 (0.2)	147.1	0.17 (0.0)	0	0.46 (0.2)	170.6	0.34 (0.1)	100	0.37 (0.1)	117.6

Table 6 continued

	LOW N NO WARM		LOW N WARM		HIGH N NO WARM		HIGH N WARM		LOW N WARM		HIGH N WARM	
	MED CO_2		MED CO_2		MED CO_2		MED CO_2		HIGH CO_2		HIGH CO_2	
	Mean (sd)	% diff	Mean (sd)	% diff	Mean (sd)	% diff	Mean (sd)	% diff	Mean (sd)	% diff	Mean (sd)	% diff
Nmin	2.8 (0.8)	−6.3	5.5 (0.7)	84.7	2.9 (0.8)	−4	5.7 (0.7)	88.3	5.5 (0.8)	82	5.5 (0.8)	83.7
strmNO$_3^-$	0.1 (0.0)	−33.3	0.1 (0.1)	−33.3	0.3 (0.0)	28.6	0.3 (0.1)	23.8	0.1 (0.0)	−38.1	0.2 (0.1)	14.3
NWT												
N-gas	0.17 (0.0)	6.3	0.30 (0.0)	87.5	0.22 (0.0)	37.5	0.35 (0.0)	118.7	0.28 (0.0)	75	0.33 (0.0)	106.3
Nmin	2.3 (0.5)	4.1	4.9 (0.8)	121	2.3 (0.6)	5.9	5.0 (0.8)	125.5	4.8 (0.8)	117.7	4.9 (0.9)	122.3
strmNO$_3^-$	0.3 (0.1)	−8.3	0.3 (0.1)	−16.7	0.7 (0.1)	91.7	0.6 (0.1)	69.4	0.3 (0.1)	−19.4	0.6 (0.1)	66.7

The mean (and standard deviation) N-gas (NO_x, N_2O, N_2) flux (N-gas, g N m^2 year^{-1}), net N mineralization rate (N_{min}, g N m^2 year^{-1}), stream NO_3^- flux (strmNO$_3^-$, g N m^2 year^{-1}), and the percent difference from base conditions from Table 2 (% diff) for the last 10 years of simulations (2065–2075) for all six scenarios

At CWT there was a 100 % decline in stream NO_3^- flux under the WARM scenario compared with NO WARM, while other sites had a more modest response. HIGH CO_2 was associated with decreased stream NO_3^- flux at HJA (young), HJA (old), NWT, and ANDCK. For most sites, stream NO_3^- fluxes were low and the absolute change in stream NO_3^- flux with scenarios was slight, but the 138 % increase under HIGH N at GRSM translated to a stream NO_3^- flux of 2.6 g N m^{-2} year^{-1} in 2075 (Table 6). With HIGH N, fluxes of stream NO_3^- at ACAD and NWT also increased by more than 50 % over baseline conditions and reached 0.3 g N m^{-2} year^{-1} or greater (Table 6). Cumulative indirect N_2O emissions from 1980 to 2075 from N leaching and runoff were proportional to stream NO_3^- leaching and ranged from a high of 27 to 29 % of direct soil N_2O emissions (186–193 g CO_2–Ce m^{-2}) under HIGH N at GRSM and a low of about 2–3 % of direct soil N_2O emissions (6–9 g CO_2–Ce m^{-2}) at the two HJA sites for all scenarios.

Net ecosystem greenhouse gas flux

Net GHG flux ranged from 13,372 g CO_2–Ce m^{-2} (HJA Young, a terrestrial sink) to −1,223 g CO_2–Ce m^{-2} at ANDCK, a terrestrial GHG source (Fig. 5). Both GRSM and ANDCRK were a source of GHGs for nearly all scenarios. In general, net ecosystem GHG sequestration was enhanced by HIGH N. For ACAD, HBR, MORA, and NWT, the net ecosystem GHG sequestration was greatest with HIGH N WARM HIGH CO_2; these sites were the three coldest forests and the colder of the two alpine sites. For other sites, CWT, GRSM, both HJA sites, and ANDCRK, the net GHG sink was greatest with HIGH N NO WARM; these sites were the warmest forests and the warmer of the two alpine sites. The least net ecosystem GHG sequestration occurred with LOW N NO WARM for the three coldest forest sites, ACAD, HBR, and MORA. The least ecosystem GHG sequestration or greatest GHG source occurred with LOW N WARM for the two alpine sites and the warmest forest sites (ANDCRK, NWT, CWT, GRSM, and both HJA sites). Among the LOW N deposition scenarios, net GHG sequestration was greatest with the WARM, HIGH CO_2 scenario, except for NWT and the two HJA sites that had greatest sequestration with NO WARM.

The rank of net carbon sequestration by site (g CO_2–Ce m^{-2}), from greatest to lowest based on the

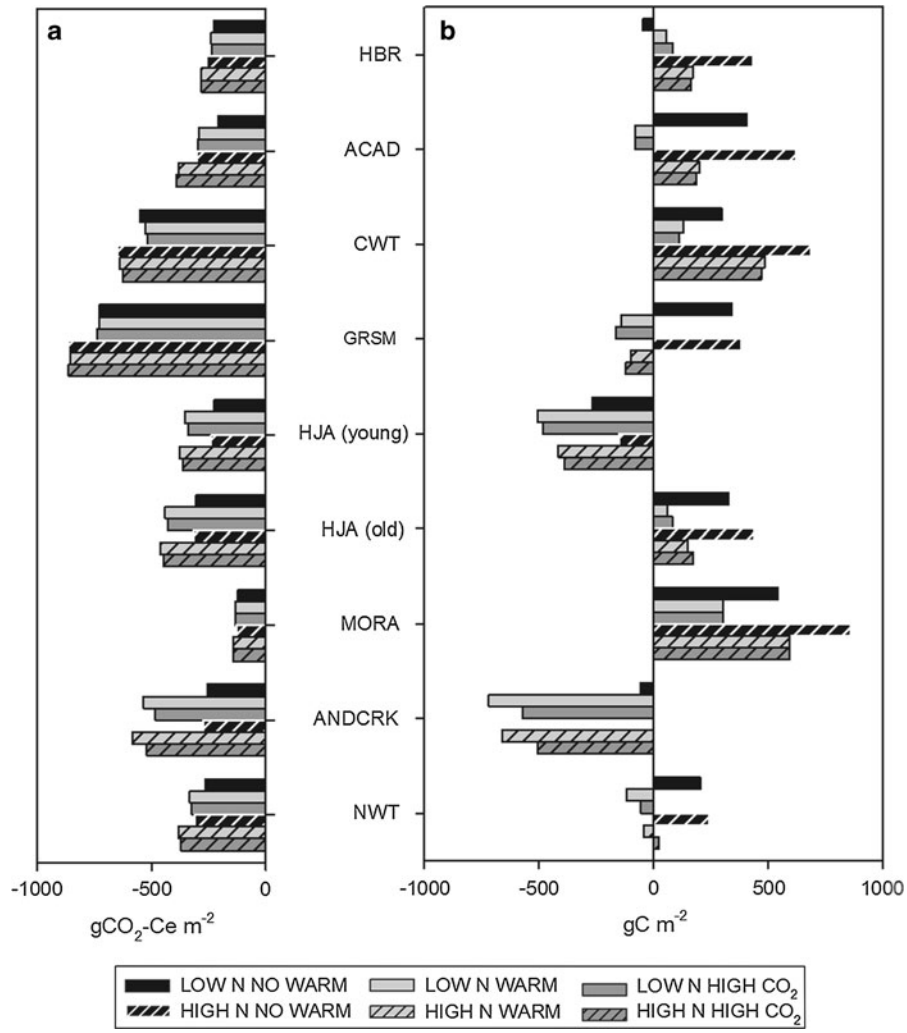

Fig. 4 Cumulative soil N_2O and carbon fluxes: **a** Cumulative N_2O emissions for 1980–2075, expressed as g CO_2–C equivalents, from direct soil N_2O and indirect N_2O from N leaching/runoff for all sites and all scenarios; **b** change in total soil organic matter carbon from 1980 to 2075 in g C m^{-2}. A negative value indicates a flux to the atmosphere or a loss from the ecosystem; a positive value indicates sequestration

average of the net balance of six scenarios was HJA (Young), HBR, HJA (Old), MORA, CWT, and ACAD. GRSM, ANDCK, and NWT were net sources of GHGs. Adding up net GHG sequestration for all sites by scenario, the model showed (in the absence of any ecologically negative effects of HIGH N on production) that net ecosystem GHG sequestration would be 49 % greater with HIGH N NO WARM than with LOW N WARM. When other factors are equal, net GHG sequestration is 7 % greater with NO WARM than with WARM, 39 % greater with HIGH N compared to LOW N, and 4–6 % greater with HIGH CO_2 concentrations vs. MEDIUM CO_2 concentrations.

The simulations showed all forests except GRSM were net sinks for GHGs under all scenarios, including LOW N WARM. The response ratios—measures of GHG sequestration where a value of 1 indicates no net gain or loss of GHGs over the 75 year simulation—for forests ranged from 0.98 (net loss of GHG) to 1.63 (net retention of GHG) with median values that ranged from 1.14 to 1.21 and were greatest when there was HIGH N (Fig. 6). In contrast, the alpine sites released a slight amount of GHGs with WARM and were unresponsive to HIGH N or HIGH CO_2 (Fig. 6). Response ratios for the alpine sites ranged from 0.86 to 1.04. The response ratio for ecosystem C for LOW N and NO WARM is of similar magnitude to the response ratios of the other treatments, indicating that the effect of a trend in CO_2 from 350 to 600 ppm over the century is strong.

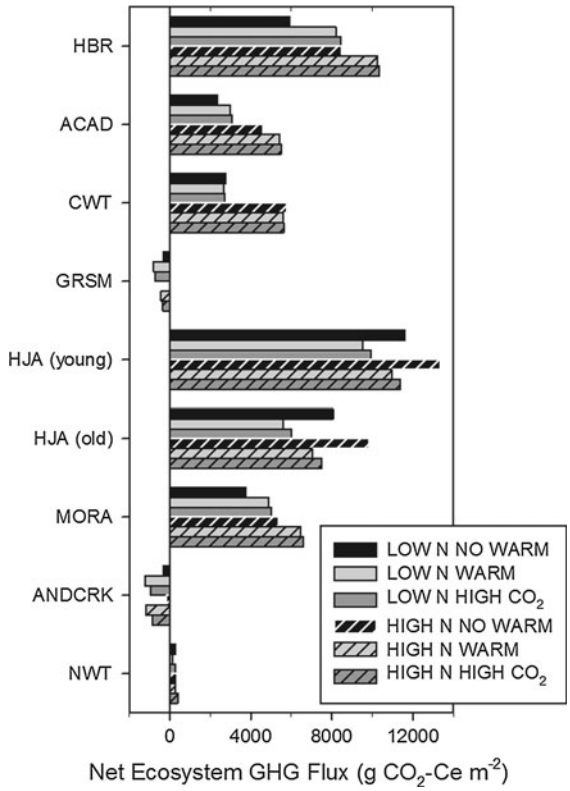

Fig. 5 The gain in ecosystem carbon from 1980 to 2075 minus cumulative direct and indirect N_2O emissions from the same time period, expressed as g CO_2–C equivalents. A negative value indicates a flux to the atmosphere or a loss from the ecosystem; a positive value indicates sequestration

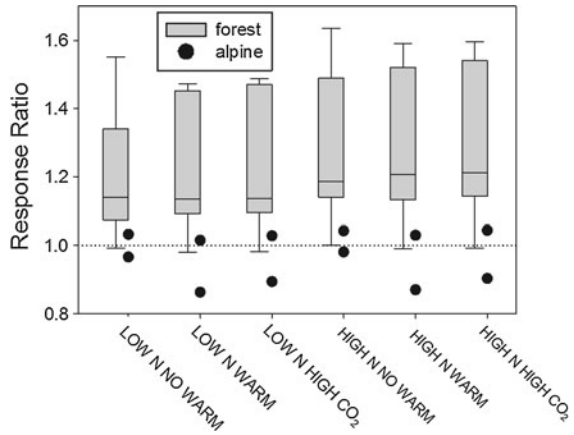

Fig. 6 The range of response ratios for forest (*box plots*) and alpine sites (*black dots*) for all scenarios. Response ratios were determined by dividing the total above- and below-ground C and soil organic matter C in 2075 (less the CO_2–C equivalent lost as direct and indirect N_2O emissions from 1980 to 2075) by the above-and below-ground C and soil organic matter C at base conditions (year 1980). For the *box plots*, the line represents the median and then the ends of the *boxes* are the 25th and 75th percentiles and the whiskers show the 10th and 90th percentiles

Discussion

There was no universal response among the forested and alpine sites we compared to N deposition, warming, or their combinations. Sites responded individually according to their vegetation type, climate, and N status. An overarching result, however, is that initial conditions with respect to N availability and mean annual temperature exert strong controls on the responses of the sites to N deposition and warming scenarios. Where initial N deposition was low, HIGH N scenarios stimulated NEP and GHG sequestration. At sites with high initial N deposition HIGH N scenarios increased stream NO_3^- fluxes. Warming stimulated ecosystem processes at those sites with the lowest mean initial annual temperatures. Warming and N deposition acted synergistically to stimulate NEP, N mineralization, and net GHG sequestration only at the colder forested sites, which were also stimulated to a lesser extent by either warming or N deposition alone.

The overall effect of CO_2 fertilization due to MEDIUM CO_2 was strong at all forested sites and one of two alpine sites, as indicated by the LOW N and NO WARM while HIGH N and WARM effects generally augmented the CO_2-induced accumulation of carbon. CO_2 fertilization effects were not enhanced substantially with the HIGH CO_2 scenario. The exceptions to this were for the alpine sites where belowground C biomass increased and stream NO_3^- fluxes decreased in the HIGH CO_2 scenarios (Fig. 1). The response ratios for the four MEDIUM CO_2 scenarios for forest sites are similar in magnitude and greater than 1.0 indicating consistent sequestration across forested sites with elevated CO_2 (Fig. 6). This CO_2 fertilization response saturated with CO_2 concentrations greater than 600 ppm. Although Earth System Models show a strong CO_2 fertilization effect when N is not limiting (Bonan and Levis 2010), we found a limited additional CO_2 response when CO_2 was increased to 760 ppm even in the presence of high N deposition. The generally limited additional response to HIGH CO_2 in this study was, in part, because endpoints of our two CO_2 scenarios (MEDIUM: 600 ppm; HIGH: 760 ppm), although realistic, were not that different from each other. Equation (1) determines that the

maximum cumulative increase in potential NPP over 75 years would be only 4.6 % greater for HIGH CO_2 than for MEDIUM CO_2. The percent increase in total biomass C (primarily belowground) at the alpine sites due to HIGH CO_2 reached this maximum potential (Fig. 1a, b). At HJA (young) and HBR the percent increase in total biomass C was half to a quarter, respectively, of this maximum potential. The model showed that the other controls on NPP (day length, temperature, self-shading, and nutrient limitation) along with ecosystem level-feedbacks to CO_2 fertilization, such as enhanced immobilization due to higher C:N in soil litter inputs, limited biomass accrual. These model results are consistent with other work that suggests that the CO_2 effect is constrained due to N and soil moisture limitation in forests and grasslands (Melillo et al. 2011; Norby et al. 2010; Pinder et al. 2012; Saleska et al. 1999).

Our model output for specific processes and locations was consistent with the results of other research. For instance, HIGH N scenarios increased aboveground C storage by 9–20 % in all forests, as also noted by others (Butterbach-Bahl et al. 2011; LeBauer and Treseder 2008; Thomas et al. 2010). The model showed that this increase in aboveground C storage came from the production of wood with high C:N ratios and long turnover times. In contrast, grasslands and foliar biomass in forests have much lower C:N ratios and thus a more limited capacity for C storage stimulated by N deposition. Liu and Greaver (2009) also found that in general N addition to grasslands does not increase C storage whereas N stimulates more C storage in forests. Warming stimulated aboveground C storage by an extra 4–19 % only in our focal forests with the lowest initial mean annual temperatures, HBR, ACAD, and MORA, and had either no or a negative effect on warmer forests (Fig. 1). Alpine sites lost aboveground C with warming. Boisvenue and Running (2006) found that warming increased forest biomass when water was not limiting. The model showed warming-induced moisture stress for HJA because growing season precipitation is low there, and for the two alpine sites that rely on snowmelt for soil moisture because warming reduced the snowpack.

DayCent-Chem showed that aboveground biomass response to increased N deposition was generally greater than the belowground response. In contrast, warming favored belowground allocation for HJA (young) and the two alpine sites. Our model results are in partial agreement with experimental and theoretical studies that suggest fine root production and root respiration decline as the plant investment for nutrient acquisition declines (Aerts and Chapin 2000; Janssens et al. 2010). Experimental studies have also shown both a strong reduction in fine root biomass with warming, consistent with the idea that warming increases N mineralization rates, and that plants allocate less C to root biomass if there is greater soil nutrient availability (Melillo et al. 2011). Our simulations support this observation that N mineralization rates were generally higher in WARM scenarios. The strong increase to belowground biomass that occurred with warming at the two alpine sites was due to warming-induced water stress that favored belowground fine root allocation over aboveground biomass allocation despite increases in N mineralization.

The greatest accumulation of SOM C at all sites occurred with HIGH N and NO WARM scenarios; warming either slowed SOM C accumulation or caused SOM C to decline (Table 4; Fig. 4). Warming increases heterotrophic respiration, which can lead to a loss of SOM C (Melillo et al. 2011), a result consistent with our model results that showed a significant increases in Rh at all sites in WARM scenarios (Table 5). Some studies have linked litter quality to a decline in SOM C in response to N addition, with measurable SOM C losses where the litter was readily decomposed, and SOM C gains with low-quality or high-lignin litter inputs (Dijkstra et al. 2004; Waldrop et al. 2004). The model showed HIGH N stimulated plant litterfall and accumulation of coarse woody debris which led to high levels of SOM C. The rates of Rh were greater for HIGH N than for LOW N (Table 5) as C and N inputs to the soil increased and as C:N ratios of plant litter decreased, but the enhanced decomposition rates of higher-quality litter did not compensate for increased litter inputs.

Published rates of NUE range 20–177 g C g N^{-1} (Pinder et al. 2012), and our NUE values fell within this range except for the two HJA forests which were substantially above it. While these two stands, with NUE above 240 g C g N^{-1}, appear to be outliers, we believe these values are appropriate. Recent published literature for Europe and North America NUE suggests values this high should be subject to suspicion (Sutton et al. 2008), but several papers for Douglas-fir forests in the Pacific Northwest that receive >1,500 mm annual precipitation describe NUE values of this

magnitude (Binkley et al. 1992; Perakis and Sinkhorn 2011). Futhermore, it is not surprising that the NUE was greatest at sites that began with the lowest measured N deposition (Fig. 3).

Net greenhouse gas sequestration

Nitrous oxide emissions that increased with warming and HIGH N dampened, and at four sites negated, the soil C sequestration ability caused by N fertilization (Fig. 4). For four of the sites (HBR, ACAD, CWT, and HJA (old)) N_2O emissions were greater than the increase in soil C storage for all warming scenarios. Nitrous oxide emissions from GRSM and NWT cancelled out long-term soil C storage for NO WARM scenarios, and N_2O emissions equaled the loss of SOM C for ANDCRK and HJA (young).

Despite the increase in N_2O emissions that came with HIGH N relative to LOW N scenarios at all but ANDCK, gains in net GHG sequestration and NEP came from the addition of N to the forested sites where increases in biomass complemented soil C changes to lead to net GHG sequestration (Fig. 5). Our simulation results are in keeping with the findings of field, modeling and meta-analysis results of experimental N additions. LeBauer and Treseder (2008) found that most ecosystems, including temperate forests and temperate grasslands, averaged 29 % growth response to N additions, which can come from N deposition (Thomas et al. 2010) or from warming-induced acceleration of the nitrogen cycle (Melillo et al. 2011). Other studies show variation in the stimulation provided by N depending on the degree of initial N limitation and on other confounding factors such as degree of soil acidification or adverse effects from ozone (Bedison and McNeil 2009; Thomas et al. 2010).

Even though cumulative net GHG sequestration from HIGH N was 40 % greater than net GHG sequestration from LOW N, the response of ecosystem C content to N additions was modest. The median forest response ratios, while almost all showing net GHG sequestration (values greater than 1), were 5–7 % greater for HIGH N compared to LOW N in our forest simulations (Fig. 6). Le Quéré et al. (2009), in their meta-analysis of US forest N-fertilization results also found on average that N addition increased ecosystem carbon content of forests by 6 %. There was no effect on net GHG sequestration in response to warming, N, or CO_2 at the alpine sites since emissions from enhanced soil organic matter decomposition and soil N_2O emissions negated any increases in above- or belowground plant C accrual.

DayCent-Chem model output reinforces the growing consensus that there will be a limited ability for continued forest or alpine GHG mitigation stimulated by N deposition or warming (Le Quéré et al. 2009; Melillo et al. 2011; Norby et al. 2010; Pinder et al. 2012; Saleska et al. 1999), and any ability may be further limited by disturbance—a factor not considered in this research except at HJA (young). Harvest or an increased amount of decomposition from fire or insect-caused mortality, can have stand-level effects on carbon uptake and storage (Hyvonen et al. 2007). Furthermore, while our simulation of HJA (young) demonstrated that forest regrowth can result in a strong GHG sink, we did not account for C emissions from harvested wood, so the total sink may be substantially lower if harvested wood is combusted or processed in emission-intensive industries. Even disturbance and regrowth will not alter the conclusion, however, that in the long run forests and alpine will provide limited capability for reduction of atmospheric CO_2 (Melillo et al. 2011).

Nitrogen mineralization and stream nitrate

Climate change and N deposition have ramifications beyond terrestrial C cycling. Our ecosystem model was developed in large part to understand how changes in terrestrial C and N processes propagate downstream to aquatic ecosystems. Nitrate in upland waters contributes to nutrient enrichment and surface water acidification, and both these drive changes to aquatic ecosystem biodiversity, productivity, and water quality (Aber et al. 2003; Baron et al. 2011). Stream NO_3^- will reflect the combined plant and soil system response to N deposition, warming, and CO_2. The residual N from above- and belowground N uptake, and microbial N cycling, particularly mineralization, immobilization, and N-gas emissions (N_2O, NO_x, and N_2), determine what gets flushed to surface waters (Aber et al. 1998). A synthesis of a data sets from the northeastern US (including HBR and ACAD), found the strongest relation of stream water NO_3^- was with N deposition alone, since heterogeneity across sites from climate variability, vegetation type, and disturbance history obscured other global

drivers (Aber et al. 2003). Likewise here we observed that although the magnitude of the effect of N deposition differed across sites, stream NO_3^- was higher at all sites in the HIGH N relative to LOW N simulations (Fig. 1). In contrast, warming and CO_2 effects on stream NO_3^- were more variable across sites underscoring the importance of N deposition as a primary driver of downstream water quality under scenarios of global change.

Watersheds with a history of high atmospheric N deposition relative to their terrestrial cycles showed strong increases in stream NO_3^- fluxes with the HIGH N scenarios. Both the greatest rate and greatest absolute increase in stream N flux occurred at GRSM, which has been N-saturated for many years (Van Miegroet et al. 2001). The strong increase of stream NO_3^- at ACAD with the HIGH N scenarios reflects the lower ability of N to be taken up in old growth spruce-fir forests on shallow soils (Hartman et al. 2009). ANDCK and NWT have received elevated N deposition and also displayed symptoms of N saturation for decades (Baron et al. 2011). With a snowmelt-dominated hydrograph, shallow soils, short growing season, and low overall plant biomass the alpine is expected to be responsive to increased N deposition. These patterns make sense since we would expect the sites with the greatest biologic stores of N to be prone to leakage of additional N inputs.

Summary and conclusions

Both GHG sequestration potential and stream water quality responses to atmospheric N deposition, climate change, and increasing atmospheric CO_2 are of interest both to scientists and to regulatory and land management agencies. DayCent-Chem simulations for diverse forest and alpine sites revealed the importance of individual site characteristics, such as plant types and climate, and their history of N deposition in their response to global change. DayCent-Chem results showed only minor differences between two levels of CO_2 fertilization and limited responses to N deposition and temperature that were similar to those reported from increasing numbers of empirical studies because of moisture, temperature, and N limitations at CO_2 concentrations greater than 600 ppm. Our results suggest N deposition could modestly strengthen the terrestrial net GHG sink primarily by increasing C stored in wood biomass of montane forests. This is countered by CO_2 emissions from accelerated soil organic carbon decomposition due to warming and increased N_2O emissions due to warming and high N deposition, reducing the overall strength of GHG storage. High N deposition did not enhance net GHG sequestration for the alpine sites or for an N-saturated forest. Warming scenarios increased net GHG sequestration only at the three coldest forested sites, and the combined effects of N deposition and warming further increased net GHG sequestration in these cold forests. While high rates of N deposition increased NO_3^- output at all sites, in scenarios with low N deposition, stream NO_3^- fluxes declined below measured values in some systems illustrating that water quality improvements could occur in the face of climate change if N deposition decreases below current amounts. DayCent-Chem model output reinforces the growing consensus that there will be a limited ability for continued forest or alpine GHG mitigation stimulated by N deposition or warming. It also illustrates that existing variability in vegetation, N deposition, and climate will play a greater role in determining the magnitude of future GHG sequestration than the differences among scenarios in N deposition, warming, and degree of CO_2 fertilization. Further, the importance of understanding linked biogeochemical cycles, their feedbacks and controls and especially their responses to global change was underscored.

Acknowledgments Funding was provided by the EPA Clean Air Markets Division, the National Park Service Air Resources Division, and the US Geological Survey. We thank Amanda Elliot Lindsey for the graphics, and Lois St. Brice for her help with the Acadia simulations. We are grateful to the editor and the anonymous reviewers for very helpful comments. This is a product of the USGS Western Mountain Initiative.

References

Aber J, McDowell W, Nadelhoffer K, Magill A, Berntson G, Kamakea M, McNulty S, Currie W, Rustad L, Fernandez I (1998) Nitrogen saturation in temperate forest ecosystems—hypotheses revisited. Bioscience 48(11):921–934

Aber JD, Goodale CL, Ollinger SV, Smith ML, Magill AH, Martin ME, Hallett RA, Stoddard JL (2003) Is nitrogen deposition altering the nitrogen status of northeastern forests? Bioscience 53(4):375–389

Aerts R, Chapin FS (2000) The mineral nutrition of wild plants revisited: A re-evaluation of processes and patterns. In:

Fitter AH, Raffaelli DG (eds) Advances in ecological research, vol 30. Advances in Ecological Research, pp 1–67
Baron JS, Ojima DS, Holland EA, Parton WJ (1994) Analysis of nitrogen saturation potential in rocky-mountain tundra and forest—implications for aquatic systems. Biogeochemistry 27(1):61–82
Baron JS, Driscoll CT, Stoddard JL, Richer EE (2011) Empirical critical loads of atmospheric nitrogen deposition for nutrient enrichment and acidification of sensitive US lakes. Bioscience 61(8):602–613
Bedison JE, McNeil BE (2009) Is the growth of temperate forest trees enhanced along an ambient nitrogen deposition gradient? Ecology 90(7):1736–1742
Binkley D, Sollins P, Bell R, Sachs D, Myrold D (1992) Biogeochemistry of adjacent conifer and alder-conifer stands. Ecology 73(6):2022–2033
Boisvenue C, Running SW (2006) Impacts of climate change on natural forest productivity: evidence since the middle of the 20th century. Glob Change Biol 12(5):862–882
Boisvenue C, Running SW (2010) Simulations show decreasing carbon stocks and potential for carbon emissions in Rocky Mountain forests over the next century. Ecol Appl 20(5): 1302–1319
Bonan GB, Levis S (2010) Quantifying carbon-nitrogen feedbacks in the Community Land Model (CLM4). Geophys Res Lett 37(7):1–6
Butterbach-Bahl K, Gundersen P, Ambus P, Augustin J, Beier C, Boeckx P, Dannenmann M, Gimeno BS, Ibrom A, Kiese R, Kitzler B, Rees RM, Smith K, Stevens C, Vesala T, Zechmeister-Boltenstern S (2011) Nitrogen processes in terrestrial ecosystems. In: Sutton M, Howard C, Erisman J, Billen G, Bleeker A, Grennfelt P, Grinsven Hv, Grizzetti B (eds) The European nitrogen assessment: sources, effects and policy perspectives. Cambridge University Press, Cambridge, pp 99–125
Campbell JL, Rustad LE, Boyer EW, Christopher SF, Driscoll CT, Fernandez IJ, Groffman PM, Houle D, Kiekbusch J, Magill AH, Mitchell MJ, Ollinger SV (2009) Consequences of climate change for biogeochemical cycling in forests of northeastern North America. Can J For Res 39(2):264–284
Canadell JG, Raupach MR (2008) Managing forests for climate change mitigation. Science 320(5882):1456–1457
Canadell JG, Le Quere C, Raupach MR, Field CB, Buitenhuis ET, Ciais P, Conway TJ, Gillett NP, Houghton RA, Marland G (2007) Contributions to accelerating atmospheric CO_2 growth from economic activity, carbon intensity, and efficiency of natural sinks. Proc Natl Acad Sci USA 104(47):18866–18870
Canham CD, Cole JJ, Lauenroth WK (2003) The role of modeling in ecosystem science. In: Canham CD, Cole JS, Lauenroth WK (eds) Models in ecosystem science. Princeton University Press, Princeton, pp 1–12
Chen BZ, Coops NC, Black TA, Jassal RS, Chen JM, Johnson M (2011) Modeling to discern nitrogen fertilization impacts on carbon sequestration in a Pacific Northwest Douglas-fir forest in the first-postfertilization year. Glob Change Biol 17(3):1442–1460
Clean Air Status and Trends Network (CASTNET) (2009) U.S. Environmental Protection Agency, Washington, D.C., http://www.epa.gov/castnet/
de Vries W, Solberg S, Dobbertin M, Sterba H, Laubhann D, van Oijen M, Evans C, Gundersen P, Kros J, Wamelink GWW, Reinds GJ, Sutton MA (2009) The impact of nitrogen deposition on carbon sequestration by European forests and heathlands. For Ecol Manag 258(8): 1814–1823
Del Grosso SJ, Parton WJ, Mosier AR, Ojima DS, Kulmala AE, Phongpan S (2000) General model for N_2O and N-2 gas emissions from soils due to dentrification. Glob Biogeochem Cycle 14(4):1045–1060
Dijkstra FA, Hobbie SE, Knops JMH, Reich PB (2004) Nitrogen deposition and plant species interact to influence soil carbon stabilization. Ecol Lett 7(12):1192–1198
Eastaugh CS, Potzelsberger E, Hasenauer H (2011) Assessing the impacts of climate change and nitrogen deposition on Norway spruce (Picea abies L. Karst) growth in Austria with BIOME-BGC. Tree Physiol 31(3):262–274
Faquhar GD (1989) Models of integrated photosynthesis of cells and leaves. Philos Trans R Soc Lond 33B:357–367
Hartman MD, Baron JS, Ojima DS (2007) Application of a coupled ecosystem-chemical equilibrium model, DayCent-Chem, to stream and soil chemistry in a Rocky Mountain watershed. Ecol Model 200(3–4):493–510
Hartman MD, Baron JS, Clow DW, Creed IF, Driscoll CT, Ewing HA, Haines BD, Knoepp J, Lajtha K, Ojima DS, Parton WJ, Renfro J, Robinson RB, Van Miegroet H, Weathers KC, Williams MW (2009) DayCent-Chem simulations of ecological and biogeochemical processes of eight mountain ecosystems in the United States. U.S. Geological Survey Scientific Investigations Report 2009–5150, p. 174
Holland EA, Dentener FJ, Braswell BH, Sulzman JM (1999) Contemporary and pre-industrial global reactive nitrogen budgets. Biogeochemistry 46(1–3):7–43
Hyvonen R, Agren GI, Linder S, Persson T, Cotrufo MF, Ekblad A, Freeman M, Grelle A, Janssens IA, Jarvis PG, Kellomaki S, Lindroth A, Loustau D, Lundmark T, Norby RJ, Oren R, Pilegaard K, Ryan MG, Sigurdsson BD, Stromgren M, van Oijen M, Wallin G (2007) The likely impact of elevated [CO_2], nitrogen deposition, increased temperature and management on carbon sequestration in temperate and boreal forest ecosystems: a literature review. New Phytol 173(3):463–480
IPCC (1996) Technical summary. In: Houghton JT, Meira Filho LG, Callander BA, Harris N, Kattenberg A, Maskell K (eds) Climate change 1995: the science of climate change: Contribution of Working Group I to the second assessment report of the Intergovernmental Panel on Climate Change. Cambridge University Press, Cambridge, pp 9–50
IPCC/WMO/UNEP (2000) Good practice guidance and uncertainty management in national greenhouse gas inventories. Intergovernmental Panel on Climate. http://www.ipcc-nggip.iges.or.jp/public/gp/bgp/4_6_Indirect_N2O_Agriculture.pdf
Janssens IA, Luyssaert S (2009) Nitrogen's carbon bonus. Nat Geosci 2(5):318–319
Janssens IA, Dieleman W, Luyssaert S, Subke JA, Reichstein M, Ceulemans R, Ciais P, Dolman AJ, Grace J, Matteucci G, Papale D, Piao SL, Schulze ED, Tang J, Law BE (2010) Reduction of forest soil respiration in response to nitrogen deposition. Nat Geosci 3(5):315–322

Lamarque JF, Kiehl JT, Brasseur GP, Butler T, Cameron-Smith P, Collins WD, Collins WJ, Granier C, Hauglustaine D, Hess PG, Holland EA, Horowitz L, Lawrence MG, McKenna D, Merilees P, Prather MJ, Rasch PJ, Rotman D, Shindell D, Thornton P (2005) Assessing future nitrogen deposition and carbon cycle feedback using a multimodel approach: analysis of nitrogen deposition. J Geophys Res-Atmos 110(D19): D19303

Le Quéré C, Raupach MR, Canadell JG, Marland G, Bopp L, Ciais P, Conway TJ, Doney SC, Feely RA, Foster P, Friedlingstein P, Gurney K, Houghton RA, House JI, Huntingford C, Levy PE, Lomas MR, Majkut J, Metzl N, Ometto JP, Peters GP, Prentice IC, Randerson JT, Running SW, Sarmiento JL, Schuster U, Sitch S, Takahashi T, Viovy N, van der Werf GR, Woodward FI (2009) Trends in the sources and sinks of carbon dioxide. Nat Geosci 2(12): 831–836

LeBauer DS, Treseder KK (2008) Nitrogen limitation of net primary productivity in terrestrial ecosystems is globally distributed. Ecology 89(2):371–379

Leung LR, Qian Y Hydrological response to climate variability, climate change, and climate extreme in the USA: climate model evaluation and projections In: Regional hydrological impacts of climatic variability and change—impact assessment and decision making. Proceedings of symposium S6 held during the Seventh IAHS Scientific Assembly. IAHS Publ., Foz do Iguaçu, Brazil 2005. vol 295. IAHS Publ.,

Leung LR, Qian Y, Bian XD, Hunt A (2003) Hydroclimate of the western United States based on observations and regional climate simulation of 1981–2000. part II: Mesoscale ENSO anomalies. J Clim 16(12):1912–1928

Liu LL, Greaver TL (2009) A review of nitrogen enrichment effects on three biogenic GHGs: the CO_2 sink may be largely offset by stimulated N_2O and CH_4 emission. Ecol Lett 12(10):1103–1117

Liu LL, Greaver TL (2010) A global perspective on belowground carbon dynamics under nitrogen enrichment. Ecol Lett 13(7):819–828

McMahon SM, Parker GG, Miller DR (2010) Evidence for a recent increase in forest growth. Proc Natl Acad Sci USA 107(8):3611–3615

McNulty SG, Aber JD, Boone RD (1991) Spatial changes in forest floor and foliar chemistry of spruce-fir forests across central New England. Biogeochemistry 14:13–29

Melillo JM, Butler S, Johnson J, Mohan J, Steudler P, Lux H, Burrows E, Bowles F, Smith R, Scott L, Vario C, Hill T, Burton A, Zhou YM, Tang J (2011) Soil warming, carbon–nitrogen interactions, and forest carbon budgets. Proc Natl Acad Sci USA 108(23):9508–9512

Nadelhoffer KJ, Emmett BA, Gundersen P, Kjonaas OJ, Koopmans CJ, Schleppi P, Tietema A, Wright RF (1999) Nitrogen deposition makes a minor contribution to carbon sequestration in temperate forests. Nature 398(6723): 145–148

Nakicenovic N et al (2000) Special report on emissions scenarios: intergovernmental panel on climate change. Cambridge University Press, New York

National Atmospheric Deposition Program/National Trends Network (NADP/NTN) (2009) Illinois State Water Survey, Urbana. http://nadp.sws.uiuc.edu/

Norby RJ, Warren JM, Iversen CM, Medlyn BE, McMurtrie RE (2010) CO(2) enhancement of forest productivity constrained by limited nitrogen availability. Proc Natl Acad Sci USA 107(45):19368–19373

Pan YD, Melillo JM, McGuire AD, Kicklighter DW, Pitelka LF, Hibbard K, Pierce LL, Running SW, Ojima DS, Parton WJ, Schimel DS, Members V (1998) Modeled responses of terrestrial ecosystems to elevated atmospheric CO(2): a comparison of simulations by the biogeochemistry models of the Vegetation/Ecosystem Modeling and Analysis Project (VEMAP). Oecologia 114(3):389–404

Parkhurst DL, Appelo CAJ (1999) User's guide to PHREEQC (Version 2)—a computer program for speciation, batch-reaction, one-dimensional transport, and inverse geochemical calculations. In: U.S. Geological Survey Water-Resources Investigations Report 99–4259, Denver, CO, pp 1–312

Parton WJ, Stewart JWB, Cole CV (1988) Dynamics of C, N, P and S in Grassland Soils: a model. Biogeochemistry 5(1):109–131

Parton WJ, Scurlock JMO, Ojima DS, Gilmanov TG, Scholes RJ, Schimel DS, Kirchner T, Menaut JC, Seastedt T, Moya EG, Kamnalrut A, Kinyamario JI (1993) Observations and modeling of biomass and soil organic-matter dynamics for the grassland biome worldwide. Glob Biogeochem Cycle 7(4):785–809

Parton WJ, Mosier AR, Ojima DS, Valentine DW, Schimel DS, Weier K, Kulmala AE (1996) Generalized model for N-2 and N_2O production from nitrification and denitrification. Glob Biogeochem Cycle 10(3):401–412

Parton WJ, Hartman M, Ojima D, Schimel D (1998) DAYCENT and its land surface submodel: description and testing. Glob Planet Change 19(1–4):35–48

Parton WJ, Holland EA, Del Grosso SJ, Hartman MD, Martin RE, Mosier AR, Ojima DS, Schimel DS (2001) Generalized model for NO_x and N_2O emissions from soils. J Geophys Res-Atmos 106(D15):17403–17419

Parton W, Silver WL, Burke IC, Grassens L, Harmon ME, Currie WS, King JY, Adair EC, Brandt LA, Hart SC, Fasth B (2007) Global-scale similarities in nitrogen release patterns during long-term decomposition. Science 315(5810): 361–364

Perakis SS, Sinkhorn ER (2011) Biogeochemistry of a temperate forest nitrogen gradient. Ecology 92(7):1481–1491

Pinder RW, Bettez ND, Bonan GB, Greaver TL, Wieder WR, Schlesinger WH, Davidson EA (2012) Impacts of human alteration of the nitrogen cycle in the US on radiative forcing. Biogeochemistry. doi:10.1007/s10533-012-9787-z

Ramaswamy V (2001) Radiative forcing of climate change. In: Houghton JT (ed) Climate change 2001: the scientific basis. Cambridge University Press, Cambridge

Saleska SR, Harte J, Torn MS (1999) The effect of experimental ecosystem warming on CO_2 fluxes in a montane meadow. Glob Change Biol 5(2):125–141

Schlesinger WH (2009) On the fate of anthropogenic nitrogen. Proc Natl Acad Sci USA 106(1):203–208

Schulze ED, Luyssaert S, Ciais P, Freibauer A, Janssens IA, Soussana JF, Smith P, Grace J, Levin I, Thiruchittampalam B, Heimann M, Dolman AJ, Valentini R, Bousquet P, Peylin P, Peters W, Rodenbeck C, Etiope G, Vuichard N,

Wattenbach M, Nabuurs GJ, Poussi Z, Nieschulze J, Gash JH, CarboEurope T (2009) Importance of methane and nitrous oxide for Europe's terrestrial greenhouse-gas balance. Nat Geosci 2(12):842–850

Sutton MA, Simpson D, Levy PE, Smith RI, Reis S, van Oijen M, de Vries W (2008) Uncertainties in the relationship between atmospheric nitrogen deposition and forest carbon sequestration. Glob Change Biol 14(9):2057–2063

Sutton MA, Oenema O, Erisman JW, Leip A, van Grinsven H, Winiwarter W (2011) Too much of a good thing. Nature 472(7342):159–161

Thomas RQ, Canham CD, Weathers KC, Goodale CL (2010) Increased tree carbon storage in response to nitrogen deposition in the US. Nat Geosci 3(1):13–17

Van Miegroet H, Creed IF, Nicholas NS, Tarboton DG, Webster KL, Shubzda J, Robinson B, Smoot J, Johnson DW, Lindberg SE, Lovett G, Nodvin S, Moore S (2001) Is there synchronicity in N input and output fluxes at the Noland Divide Watershed, a small N-saturated forested catchment in the Southern Appalachians? Sci World S2:480–492

Waldrop MP, Zak DR, Sinsabaugh RL (2004) Microbial community response to nitrogen deposition in northern forest ecosystems. Soil Biol Biochem 36(9):1443–1451

Zaehle S, Ciais P, Friend AD, Prieur V (2011) Carbon benefits of anthropogenic reactive nitrogen offset by nitrous oxide emissions. Nat Geosci 4(9):601–605